

1 **Paleotethyan evolution of the Indochina Block as deduced from**
2
3 **granites in northern Laos**
4

5
6 Shifeng Wang^a, Yasi Mo^b, Chao Wang^b, and Peisheng Ye^a
7
8

9
10
11 a Institute of Geomechanics, Chinese Academy of Geological Sciences, Beijing
12

13
14 100081, China;
15

16
17 b Institute of Tibetan Plateau Research, Chinese Academy of Sciences, Beijing
18

19
20 100101, China
21
22
23
24

25 **Abstract:** Increasing level of details about the Paleotethyan evolution of the SE
26
27 Asia have been defined in recent years. Questions remain, however, over the role of
28
29 the Dien Bien Phu Suture Zone in the evolution of the Indochina block and whether
30
31 the Song Ma Suture represents the boundary between the Indochina block and the
32
33 South China Block; such debate extends to their plate convergence geometry prior to
34
35 collision. Granitoid geochronological and geochemical data obtained in northern Laos
36
37 provide new information *vis-à-vis* these arguments. Zircon U-Pb ages together with
38
39 whole rock, trace and rare earth element data from 27 granitic rocks from five
40
41 complexes allow us to conclude that these granites are typical of I-type Indosinian
42
43 volcanic arc granites. However, the 234-256Ma I-type granites mismatch the initiation
44
45 age obtained from the ductile shear zone of the Dien Bien Phu Fault, thus repudiating
46
47 the existence of the Dien Bien Phu Suture Zone. This then implies that the
48
49 Qamdo-Simao and Indochina blocks were united. Zircon inheritance ages and zircon
50
51
52
53
54
55
56
57
58
59
60

1 crustal two-stage model ages suggest that the main crust in the Indochina Block
2
3 formed in the Late Paleoproterozoic to Early Mesoproterozoic, much later than the
4
5 Archean crustal formation age identified east of the Song Ma Suture. Moreover, the
6
7 440–404Ma and 234–256Ma I-type granites suggest that the boundary between
8
9 Indochina and South China should be the Jinsha River Suture-Song Ma
10
11 Suture-Kontum Massif, instead of the Jinsha River Suture-Song Chay Suture. Finally,
12
13 the Emeishan basalt and granite complexes both form part of the South China tectonic
14
15 units subducting westward (or southward in a palaeogeographic sense) under the
16
17 Qamdo-Simao and Indochina blocks.
18
19
20
21
22
23
24
25
26
27

28 **Keywords:** granite; Laos; zircon U-Pb age; Lu-Hf; whole-rock major, trace and rare
29
30 earth elements
31
32
33
34
35

36 **1. Introduction**

37
38

39 Mainland SE Asia is formed of several micro-continent (*e.g.* the Sibumasu,
40
41 Indochina, Qamdo-Simao and South China blocks) which amalgamated during the
42
43 closure of the Paleotethyan Ocean from the Late Permian to the Early Triassic (*e.g.*
44
45 Sengor, 1979; Metcalfe 1996, 1999, 2002, 2013; Lepvrier *et al.*, 2004, 2008; Carter *et*
46
47 *al.*, 2001; Ueno, 2003; Ferrari *et al.*, 2008; Liu *et al.*, 2012; Faure *et al.*, 2014). A long
48
49 S-N trending line of ophiolitic mélangé suites, forming part of the Paleotethys Suture
50
51 Zone, can be followed from the Malaysian Peninsula in the south to southwestern
52
53 China in the north (Fig. 1). These are the Bentong-Raub Suture in the Malaysian
54
55
56
57
58
59
60
61
62
63
64
65

1 Peninsula, the parallel Inthanon Suture and Nan-Uttaradit Sutures in north-central
2
3 Thailand, the so-called Dien Bien Phu Suture in Laos and Vietnam (where the Dien
4
5 Bien Phu fault is developed) and the Changning-Menglian Suture in China (*e.g.*
6
7 Hutchison, 1975; Barr and MacDonald, 1987; Barr *et al.*, 2000; Wu *et al.*, 1995;
8
9 Singharajwarapan and Berry., 2000; Sone and Metcalfe, 2008). A granitoid belt is
10
11 distributed parallel to the Paleotethys Suture. The age of the granitoids in the granitoid
12
13 belt ranges from 265 to 230Ma (*e.g.* Beckinsale *et al.*, 1979; Liew and McCulloch,
14
15 1985; Barr *et al.*, 2000; Searle *et al.*, 2012; Gardiner *et al.*, 2015), the same age as the
16
17 blueschist facies metamorphic rocks that are in association with the Paleotethys
18
19 Suture (*e.g.* Barr and MacDonald, 1987; Singharajwarapan and Berry., 2000).
20
21 Conversely, radiometric dating of syn-tectonic high-pressure metamorphic rocks (*e.g.*
22
23 Lepvrier *et al.*, 1997, 2004; Lan *et al.*, 2003; Osanai *et al.*, 2001, 2004; Nakano *et al.*,
24
25 2007) and Indosinian granitoid (*e.g.* Nagy *et al.*, 2001; Lan *et al.*, 2000; Owada *et al.*,
26
27 2007; Sanematsu *et al.*, 2011) in Vietnam, including in the Truong Son Belt and the
28
29 Kontum Massif of central-southwestern Vietnam, has recorded Indosinian orogeny
30
31 within a restricted time interval between $258\pm 6.6\text{Ma}$ and $243\pm 6.5\text{Ma}$. The Late
32
33 Permian to Early Triassic coeval events in Southeast Asia are broadly accepted as
34
35 indicating the initial subduction between the Sibumasu-Indochina and South China
36
37 blocks.
38
39
40
41
42
43
44
45
46
47
48
49
50
51
52

53 Despite some progress, arguments remain about the welding of the blocks in
54
55 Southeast Asia. For example, new progress confirm that the Changning–Menglian and
56
57 Inthanon suture zones are regarded as the Palaeo-Tethys Suture Zone, the
58
59
60
61
62
63
64
65

1 Jinghong-Luang Prabang-Nan-Sra Kaeo suture is regarded as a closed back-arc basin
2
3 (e.g. Sone and Metcalfe, 2008; Metcalfe, 2011, 2013; Qian et al., 2015). Uncertainty
4
5 exists about the role of the Dien Bien Phu suture in the Paleotethys evolution of the
6
7 SE Asia (Fig. 1). Establishing this would help determine whether the Qamdo-Simao
8
9 Block is part of the Indochina Block, or if the Indochina and the Qamdo-Simao blocks
10
11 are two separate blocks. This question has perplexed geologists for a long time (e.g.
12
13 Metcalfe, 1996, 2002, 2006; Wang *et al.*, 2000; Carter *et al.*, 2001). One view insists
14
15 that the Sukhothai Arc and the Inthanon Suture correlate with the Lincang-Jinghong
16
17 Volcanic Belt and the Changning-Menglian Suture in Yunnan, China (e.g. Sone and
18
19 Metcalfe, 2008; Metcalfe, 2011, 2013). Taking this view, the Qiangtang-Baoshan
20
21 Block west of the suture would form the northern part of the Sibumasu Continent, and
22
23 the Qamdo-Simao Block east of the suture would represent the northern continuity of
24
25 the Indochina Continent (e.g. Wang *et al.*, 2000; Carter *et al.*, 2001; Carter and Clift,
26
27 2008; Ferrari *et al.*, 2008; Liu et al., 2012; Faure et al., 2014); But others argue that
28
29 the Nan-Uttaradit Suture bends northeastward at the Dien Bien Phu Segment and joins
30
31 the Song Ma Suture, separating the Nan-Uttaradit Suture from the
32
33 Changning-Menglian Suture by hundreds of kilometers (Sengor, 1979; Leloup *et al.*,
34
35 1995; Singharajwarapan and Berry., 2000; Lepvrier *et al.*, 2004, 2008). Another
36
37 question concerns the time and geometry of plate convergence prior to collision
38
39 between the Indochina and the South China blocks. Paleogeographic evidence
40
41 suggests a connection between Indochina and South China up to the Carboniferous
42
43 (e.g. Hutchison, 1989; Janvier *et al.*, 1997; Racheboeuf *et al.*, 2005, 2006; Metcalfe,
44
45
46
47
48
49
50
51
52
53
54
55
56
57
58
59
60
61
62
63
64
65

1 1996, 2002, 2013), but syn-tectonic magmatic and metamorphic data show a
2
3 tectono-thermal event that occurred between 260Ma and 240Ma (*e.g.* Lepvrier *et al.*,
4
5
6 1997, 2004, 2008, 2011; Nagy *et al.*, 2001; Lan *et al.*, 2000, 2003; Owada *et al.*, 2007;
7
8
9 Nakano *et al.*, 2007; Sanematsu *et al.*, 2011; Lai *et al.*, 2014). Additionally, varying
10
11 opinions about the geometry of block convergence prior to collision exist, and include:
12
13
14 1) the eastward subduction of the Indochina Block beneath the South China Block
15
16 (Lepvrier *et al.*, 1997, 2004; Lan *et al.*, 2000); 2) the westward (or southward in a
17
18 palaeogeographic sense, the same below) subduction of the South China Block
19
20 beneath the Indochina Block (Liu *et al.*, 2012; Faure *et al.*, 2014); and 3) the existence
21
22 of a pair of subduction zones dipping in opposite directions (Lepvrier *et al.*, 2008).
23
24
25
26
27

28 Most areas of Laos are covered by virgin forest, which makes tracking the
29
30 outcrops of the Dien Bien Phu ophiolitic suture difficult. Fortunately, granitoids are
31
32 distributed broadly along the road from Phonsavan to Sam Neua in northern Laos,
33
34 south of the junction between the Dien Bien Phu Suture and the Song Ma Suture (Fig.
35
36
37 2). It is widely accepted that the geochronological and geochemical data of granitic
38
39 rocks can provide important information regarding the crustal evolution of tectonic
40
41 plates. The geochronology and geochemistry of granitic rocks in northern Laos,
42
43 however, is poorly known, due to their inaccessibility. In recent years we have
44
45 collected more than 100 samples from different granitoid complexes in northern Laos
46
47 in order to reconstruct the convergence process of Southeast Asian blocks during the
48
49 closure of the Paleotethyan Ocean.
50
51
52
53
54
55
56
57

58 **2. Geological setting**

59
60
61
62
63
64
65

2.1 The rocks in northern Laos

Proterozoic to Quaternary strata outcrop in central-northern Laos (Department of Geology and Mine, Lao P. D. R. (DGM), 1991; Fig. 2), and can be divided into three main units: Late Palaeozoic, Early Mesozoic and Late Mesozoic. Late Palaeozoic strata are mainly shallow sea shelf sequences interbedded with volcano-sedimentary sequences, mostly of sandstone, siltstone and shale. There are a few outcrops of Early Palaeozoic rocks, which are mainly deep-water, marine volcano-sedimentary, metamorphosed to low or low-medium grades (DGM, 1991). Early Mesozoic strata are mostly of continental rock, with local shallow-water marine facies. Rocks in this unit are red argillaceous sandstone, with occasional thin coal seams and conglomerates. These two stratigraphic units are distributed in a N-S direction. Late Mesozoic strata are mainly confined to the Vientiane Basin; rocks are mainly red continental sandstones and clays, with lagoonal mud rocks in the upper levels bearing evaporate rocks of halite and gypsum. Granitoid complexes have developed on the Xieng Khoang Plateau of northern Laos (Fig.2), which is located at the junction of the N-S trending granitoid belt at the Dien Bien Phu Segment of the Nan and Dien Bien Phu suture zones and the NW-striking Truong Son Belt. The granitoid belt along the Nan Suture has been interpreted being composed of syn-tectonic granitoids from the subduction of the Sibumasu Continent eastward into Indochina (*e.g.* Beckinsale *et al.*, 1979; Charusiri *et al.*, 1993; Barr *et al.*, 2000). Conversely, the granitoids located along the northwestern extension of the Truong Son Belt have been attributed to the syn-tectonic or within-plate granitoids of the Indochina Block during its subduction

1 eastward under the South China Block (*e.g.* Lepvrier *et al.*, 1997, 2004; Sanematsu *et*
2
3 *al.*, 2011).
4

5 6 **2.2 The tectonic setting around northern Laos**

7 8 9 **2.2.1 The Nan and Dien Bien Phu Suture Zones**

10
11 The magmatic and sedimentary rocks in northern Laos are confined by two
12 tectonic boundaries: the Nan-Dien Bien Phu Suture Zone in the west and northwest,
13 and the Truong Son Belt in the east. The S-N striking Nan Suture Zone west of Laos
14 consists of a belt of ophiolitic mafic and ultramafic rocks formed in a back-arc or
15 inter-arc setting (Barr and MacDonald, 1987; Barr *et al.*, 2000; Singharajwarapan,
16 2000), accompanied by metasedimentary rocks of the Sukhothai Fold Belt and
17 syn-tectonic granite defined as a granite belt (Sone and Metcalfe, 2008). Northward,
18 the suture bends eastward and joins with the Song Ma Suture, thus separating the
19 Indochina Block from the Qamdo-Simao Block (Sengor, 1979; Leloup *et al.*, 1995;
20 Singharajwarapan and Berry, 2000). Alternatively, the Nan Suture could connect
21 northward with the Jinghong Suture in Yunnan, China (*e.g.* Bar *et al.*, 1987, 2000;
22 Wu *et al.*, 1995; Sone and Metcalfe, 2008).
23
24
25
26
27
28
29
30
31
32
33
34
35
36
37
38
39
40
41
42
43
44

45 **2.2.2 Tectonic units from Inner Indochina to the Red River Fault**

46
47 The Song Ma Suture defines the boundary between the Indochina and South
48 China blocks, although the Song Da or Song Chay sutures have also been considered
49 the boundary (*e.g.* Lepvrier *et al.*, 2004; Liu *et al.*, 2012; Faure *et al.*, 2014). Eastward,
50 the tectonic units from inner Indochina to South China can be subdivided into: the
51 Indochina Basement; the Song Ma Suture Zone; the Nam Co Complex; the Song Da
52
53
54
55
56
57
58
59
60
61
62
63
64
65

1 Rift Zone; the Tu Le Basin and the Song Chay Suture Zone (dissected by the Red
2
3 River Fault (RRF) during the Cenozoic). The features of these tectonic units are
4
5 described below; the relations between the units are shown as a simplified section in
6
7
8
9 Figure 3.

10
11 1) The Indochina Basement. Some high-grade metamorphic rocks and granite
12
13 complexes in northern Laos and northwestern Vietnam are attributed to the Archean
14
15 to Proterozoic eons (DGM, 1991; Department of Geological and Minerals of Vietnam
16
17 (DGMV), 2005), similar to the basement of the Kontum Massif in the southernmost
18
19 part of Vietnam (*e.g.* Osanai *et al.*, 2001, 2004; Owada *et al.*, 2007; Nakano *et al.*,
20
21 2007; Sanematsu *et al.*, 2011);
22
23
24
25
26
27

28 2) The Song Ma Suture Zone, which is composed of Song Ca volcanic arc, the
29
30 Truong Son Belt (Truong Son arc granitoids) and the Song Ma tectonic mélange from
31
32 W-E. The Song Ca volcanic arc is comprised mainly of a sequence of calcalkaline
33
34 volcanic associations of ages 270–248Ma, using $^{40}\text{Ar}/^{39}\text{Ar}$ dating (Lan *et al.*, 2003).
35
36
37 The Truong Son Belt consists of widespread Late Paleozoic to Early Mesozoic
38
39 intrusions. Truong Son Belt strata exhibit: Neoproterozoic high-grade metamorphic
40
41 rocks; Silurian to Lower Devonian and Upper Permian marine sedimentary rocks;
42
43 Upper Permian basalt, amygdaloidal basalt and tuffs; and Triassic marine and
44
45 terrigenous sedimentary rocks. The Song Ma mélange is defined as the boundary
46
47
48 between the Indochina and South China blocks that occurred during the westward
49
50 subduction of the South China Sea under the Indochina Block in the Later Permian to
51
52
53 Early Triassic (*e.g.* Lepvrier *et al.*, 2004, 2008; Liu *et al.*, 2012; Faure *et al.*, 2014). It
54
55
56
57
58
59
60
61
62
63
64
65

1 consists of sheets of rocks with ages from Neoproterozoic to Early Triassic. These
2
3 rocks are highly sheared, juxtaposed by shear zones and intruded by gabbro,
4
5
6 plagiogranite, granodiorite and granite (DGMV, 2005).
7

8
9 3) The Nam Co complex, a high-grade metamorphic massif. Proterozoic
10
11 greenschist to amphibolite facies metamorphic rocks, including gneisses, schists,
12
13 amphibolites, quartzite and marbles constitute the majority of the massif. The
14
15 metamorphic rocks are highly foliated and lineated, and formed ca. 245Ma (Lepvrier,
16
17 *et al.*, 2004).
18
19
20
21

22
23 4) The Song Da Rift Zone. The lowermost sequence is composed of Lower
24
25 Permian carbonates overlain by a sequence of mafic to ultramafic volcanic rocks of
26
27 the Lower Permian Cam Thuy Formation. The middle sequence is Upper Permian to
28
29 Early Triassic, and is composed of an association of komatiite-basalt, trachytic basalt,
30
31 trachytic andesite and trachytic dacite . Upward, the sequence exhibits calcareous
32
33 sediments interlayered with felsic volcanics in its Mid to Late Triassic sediments. The
34
35 top sequence is Cretaceous sedimentary rocks unconformably overlying old
36
37 sequences. East of the Song Da Rift Zone is the Tu Le Basin, which is filled with
38
39 Mesozoic continental sediments. East of the Tu Le Basin is the Song Chay Suture
40
41 Zone, which includes the Song Chay ophiolitic mélange and the Day Nui Con Voi
42
43 (DNCV) gneiss belt, where the Red River Fault dissected the mélange during the
44
45 Cenozoic.
46
47
48
49
50
51
52
53

54
55 The Indochina block has been thoroughly overprinted and cut by Neogene
56
57 strike-slip faults such as the Ailaoshan-Red River Fault, the Wangchao Fault and the
58
59
60

1 Dien Bien Phu Fault. The NE-trending Dien Bien Phu Fault in the study area was the
2
3 southernmost segment of the Xianshuihe fault system during the Late Cenozoic; the
4
5 fault has been an active left-lateral strike slip fault since ca. 5.5Ma, and reactivated
6
7 after 228Ma or 198-158Ma with totally 30-40km right-lateral offset accumulated (*e.g.*
8
9 Wang *et al.*, 1998; Zuchiewicz *et al.*, 2004; Koszowska *et al.*, 2007; Lin *et al.*, 2009;
10
11 Roger *et al.*, 2014).
12
13
14
15

16 17 **3. Analytical method** 18 19

20 About 24 granite samples were prepared for zircon U-Pb LA-ICP-MS dating.
21
22 Zircons were separated using conventional heavy-liquid and magnetic techniques.
23
24 Pure zircon grains were selected using a binocular microscope. Representative grains
25
26 were placed into an epoxy resin, along with several standard transmission electron
27
28 microscopy (TEM) samples, and ground down by about half to expose the zircon
29
30 interior, before performing U-Pb dating. Before and after the dating, the transmitted
31
32 and reflected light were analyzed using a microscope and backscattering images,
33
34 together with cathode luminescence images, in order to determine crystalline shape,
35
36 inner structure and dating position.
37
38
39
40
41
42
43

44 U-Pb dating of zircons was conducted using a New Wave UP193FX Excimer
45
46 laser, coupled with an Agilent 7500a ICPMS, at the Key Laboratory of Continental
47
48 Collision and Plateau Uplift, Institute of Tibetan Plateau Research, Chinese Academy
49
50 of Sciences (CAS), Beijing. The diameter of the laser beam was 36mm, and the
51
52 duration of ablation was 45s. Zircon standard 91500 was used as an external standard
53
54 to correct isotopic ratios. TEM characterization of zircon was used to monitor results.
55
56
57
58
59
60
61
62
63
64
65

1 Concentrations of the elements were calculated using NIST612 glass as the external
2
3 standard and ^{29}Si as the internal standard. Age data were processed using Glitter 4.4
4
5 software (details can be found in Jackson *et al.*, 2004). Diagrams were produced using
6
7 the Isoplot 3.0 Toolkit (Ludwig, 2003).
8
9

10
11 *In-situ* Hf isotope analysis was performed on zircon grains using LAICPMS with
12
13 a beam size of $60\mu\text{m}$ and a laser pulse frequency of 8Hz. Details of instrument
14
15 conditions and data acquisition are given in Wu *et al.* (2006) and Xie *et al.* (2008).
16
17 During the analysis, $^{176}\text{Hf}/^{177}\text{Hf}$ ratios of the zircon standard (91500) were
18
19 0.282286 ± 12 (2σ , $n=21$). The $\epsilon\text{Hf}(t)$ values (parts in 10⁴ deviations in initial Hf
20
21 isotope ratios between the zircon sample and the chondritic reservoir) and T_{DM2}
22
23 (zircon Hf isotope crustal model ages based on a depleted-mantle source and an
24
25 assumption that the protolith of the zircon's host magma has a mean continental
26
27 crustal $^{176}\text{Lu}/^{177}\text{Hf}$ ratio of 0.015) were calculated following Griffin *et al.* (2002),
28
29 using the ^{176}Lu decay constant given in Blichert-Toft and Albarède (1997).
30
31
32
33
34
35
36
37
38

39 About six granite samples were chosen for whole-rock major, rare earth and
40
41 trace element analysis. Samples for elemental analysis were powdered to $<20\mu\text{m}$
42
43 using an agate mill. Major element analyses were conducted at the Institute of
44
45 Geology and Geophysics, CAS. Major element abundances (wt.%) of whole-rock
46
47 samples were determined using a Phillips PW X-ray fluorescence spectrometer
48
49 (XFR-2400) and yielded an analytical uncertainty of $<5\%$ ($\pm 1\sigma$). Rare earth and other
50
51 trace elements were analyzed using ICP-MS techniques at the Institute of Tibetan
52
53 Plateau Research, CAS. The detailed operating conditions for the laser ablation
54
55
56
57
58
59
60
61
62
63
64
65

1 system, the ICP-MS instrument and data reduction were the same as those described
2
3 by Liu *et al.* (2008), with the uncertainties for all elements <5%.
4
5
6
7

8 **4 Results**

9 **4.1 U-Pb dating**

10
11
12 More than 40 samples from six granite complexes along the road from
13
14 Phonsavan to Sam Neua in northern Laos were selected for zircon analysis, and ca. 20
15
16 representative samples are presented in this paper to show the geochronology of the
17
18 complexes. The samples collected are termed LC-1, LC-6 and LC-8 (from the Lat
19
20 Boua Complex), LC-12, LC-16 and LC-17 (from the Kham Complex), LH-1, LH-4
21
22 and LH-5 (from the Phon Thong Complex), LH-11, LH-13 and LH-16 (from the Luu
23
24 Complex), LT-1, LT-3, LT-4 and LT-6 (from the Na The Complex), and LB-3, LB-5,
25
26 LB-6 and LB-7 (from the Laosang Complex) (Fig. 2). The sites of the complexes are
27
28 located between 19°41.396'N to 20°49.650'N, and 103°28.176'E to 104°19.781'E. Of
29
30 the six complexes, the Lat Boua, Kham, Phon Thong, Luu and Na The complexes
31
32 exhibit ages ca. 234–256Ma; the Laosang Complex gives a mean age of 420Ma (Fig.
33
34 4, Table 1 in Appendix A). Only a few zircons from some samples show the existence
35
36 of inherited cores as described in Section 4.2 and Table 2 in Appendix B.
37
38
39
40
41
42
43
44
45
46
47
48
49

50 Zircon from the 16 samples from the Lat Boua, Kham, Phon Thong, Luu and
51
52 Na The complexes are mainly light yellow to transparent, euhedral prismatic grains.
53
54 Cathode luminescence images (CL) show that these zircons generally have
55
56 luminescent (low U) cores with euhedral fine-scale oscillatory igneous zoning. They
57
58
59
60
61
62
63
64
65

1 generally range from 120–200µm in length and 50–80µm in width. As a rule, we
2
3 selected 25-35 representative zircons from these 16 samples for U-Pb dating (Table 1
4
5 in Appendix A). Th/U ratios range from 0.18 to 1.58, indicating a typical magmatic
6
7 origin. Analytical results generally group together and yield weighted mean $^{206}\text{Pb}/^{238}\text{U}$
8
9 ages ranging from 234.3±1.5Ma to 256.4±3.1Ma (95% confidence; MSWD values
10
11 range from 0.9 to 1.5) (Fig. 4), which we interpret as the crystallization ages of the
12
13 Lat Boua, Kham, Phon Thong, Luu and Na The complexes.
14
15
16
17
18
19

20 The Laosang granite complex, where samples LB-3, LB-5, LB-6 and LB-7 were
21
22 collected, is located at approximately 19°13.872'N, 103°40.482'E. Zircons from
23
24 samples LB-3, LB-5, LB-6 and LB-7 consist of light yellow to transparent, euhedral
25
26 prismatic grains. CL images show that these zircons generally have luminescent (low
27
28 U) cores with euhedral fine-scale oscillatory igneous zoning. They generally range
29
30 from 120–180µm in length and 50–80µm in width. Zircon characteristics are similar
31
32 to those of zircon from the other five complexes. We selected 30, 22, 25 and 26
33
34 representative zircons respectively from the four samples for U-Pb dating (Table 1 in
35
36 Appendix A). The Th/U ratios range from 0.18 to 1.58, 0.20 to 2.06, 0.16 to 1.30 and
37
38 0.18 to 0.76, respectively, indicating typical magmatic origins. Analytical results
39
40 gained generally group together and yield a weighted mean $^{206}\text{Pb}/^{238}\text{U}$ age of
41
42 431.4±2.6Ma (95% confidence, MSWD=1.5) from LB-3, 425.4±2.4Ma from LB-5
43
44 (95% confidence, MSWD=0.5), 435.1±3.8Ma from LB-6 (95% confidence,
45
46 MSWD=1.0) and 402.5±1.9Ma (95% confidence, MSWD=1.8) from LB-7 (Figs. 4q,
47
48 4r, 4s, 4t), which we interpret as the crystallization ages of the Laosang granite
49
50
51
52
53
54
55
56
57
58
59
60
61
62
63
64
65

1 complex.
2
3
4
5

6 **4.2 Zircon Lu-Hf isotopic data** 7

8
9 We selected a total of 12 samples, *i.e.* LC-1, LC-8, LC-12, LC-17, LH-4, LH-5,
10 LH-11, LH-16, LT4, LT6, LB-5 and LB-7, for *in-situ* Lu-Hf isotopic analyses based
11 on zircon U-Pb dated samples of the six complexes described in section 4.1.
12
13 Approximately 15-20 spots in each sample (totally 201 spots) were selected for
14 analysis. The results are listed in Table 2 in Appendix B and shown in Figure 5.
15
16
17
18
19
20
21

22 The 31 analyses of protogenetic magmatic zircon from the Lat Boua Complex
23 display initial $^{176}\text{Hf}/^{177}\text{Hf}$ ratios ranging from 0.282075 to 0.282644, and $\epsilon\text{Hf}(t)$ values
24 from -19.1 to 0.9, with only spot LC-8-6 having a positive $\epsilon\text{Hf}(t)$ value.
25
26 Corresponding Hf crustal two stage model ages (T_{DM2}) range from 1218Ma to
27
28 1701Ma, with a mean of 1526 Ma. The 29 analyses of young U-Pb ages from the
29
30 Kham Complex display initial $^{176}\text{Hf}/^{177}\text{Hf}$ ratios ranging from 0.282336 to
31
32 0.282604 and $\epsilon\text{Hf}(t)$ values from -9.5 to -0.5; corresponding Hf crustal T_{DM2} ages
33
34 range from 1218Ma to 1701Ma, with a mean of 16984Ma. The 37 analyses from the
35
36 Phon Thong Complex display initial $^{176}\text{Hf}/^{177}\text{Hf}$ ratios ranging from 0.282369 to
37
38 0.282632, $\epsilon\text{Hf}(t)$ values from -8.9 to 0.4, and Hf crustal T_{DM2} ages from 1245Ma to
39
40 1835Ma, with a mean of 1606Ma. 21 spots from the Luu Complex show initial
41
42 $^{176}\text{Hf}/^{177}\text{Hf}$ ratios ranging from 0.281943 to 0.282687 and $\epsilon\text{Hf}(t)$ values from -24.0
43
44 to 2.5, with only spot LH-4-13 having a positive $\epsilon\text{Hf}(t)$ value; Hf crustal T_{DM2} ages
45
46 range from 1120Ma to 2789Ma, with a mean of 1679 Ma. The 33 isotopic analyses of
47
48
49
50
51
52
53
54
55
56
57
58
59
60
61
62
63
64
65

1 the Na The Complex display initial $^{176}\text{Hf}/^{177}\text{Hf}$ ratios ranging from 0.282333 to
2
3 0.282636 and $\epsilon\text{Hf}(t)$ values from -9.9 to 0.5 (only spot LT-4-18 has a positive value),
4
5 with a mean value of -4.6; Hf crustal T_{DM2} ages range from 1240Ma to 1909Ma, with
6
7 a mean of 1574Ma. The 38 analyses from the Laosang Complex display initial
8
9 $^{176}\text{Hf}/^{177}\text{Hf}$ ratios ranging from 0.282283 to 0.282540, $\epsilon\text{Hf}(t)$ values from -8.1 to
10
11 1.2 (only spot LB-5-17 has a positive value), and Hf crustal T_{DM2} ages from 1220Ma
12
13 to 2751Ma, with a mean of 1678Ma. These Lu-Hf isotopic features obtained from
14
15 protogenetic magmatic zircons indicate that the rock formations of the complexes
16
17 were principally resourced from the Late Paleoproterozoic to Early Mesoproterozoic
18
19 continental crust, with a minute quantity from the depleted mantle.
20
21
22
23
24
25
26
27

28 Besides the analyses of protogenetic magmatic zircons, Hf crustal T_{DM2} ages
29
30 were recorded using inherited zircons in four complexes, *i.e.* the Lat Boua, Kham,
31
32 Luu and Laosang complexes. The U-Pb ages of two inherited zircons from spots
33
34 LC-8-2 and LC-8-15 in the Lat Boua Complex are 667Ma and 892Ma, respectively;
35
36 their $^{176}\text{Hf}/^{177}\text{Hf}$ ratios are 0.282844 and 0.282944, their $\epsilon\text{Hf}(t)$ values are 4.9 and
37
38 6.8, and they exhibit corresponding T_{DM2} values of 1336 and 1288Ma, respectively. In
39
40 the LC-12 sample from the Kham Complex, the U-Pb ages of two inherited zircons
41
42 from spots LC-12-6 and LC-12-12 are 530Ma and 580Ma, respectively; their
43
44 $^{176}\text{Hf}/^{177}\text{Hf}$ ratios are 0.282366 and 0.282049, their $\epsilon\text{Hf}(t)$ values are -9.2 and -11.0,
45
46 and they give corresponding T_{DM2} values of 2070 and 2222Ma, respectively. In the
47
48 LC-17 sample, the U-Pb ages of the five inherited zircons are 440Ma, 750Ma, 618Ma,
49
50 822Ma and 915Ma, respectively; their $^{176}\text{Hf}/^{177}\text{Hf}$ ratios range from 0.282140 to
51
52
53
54
55
56
57
58
59
60
61
62
63
64
65

0.282573, their mean $\epsilon\text{Hf}(t)$ value is -6.0, and corresponding T_{DM2} values lie between 1710Ma and 2446Ma. In the LB-5 sample from the Laosang Complex, the U-Pb ages of three inherited zircons from spots LB-5-6, LB-5-16 and LB-5-19 are 645Ma, 1367Ma and 515Ma respectively; their $^{176}\text{Hf}/^{177}\text{Hf}$ ratios are 0.282103, 0.282453 and 0.282345, their $\epsilon\text{Hf}(t)$ values are -13.1, -1.7 and -6.0, and their corresponding T_{DM2} values are 1860, 2233 and 2408Ma, respectively. In the LB-7 sample, the U-Pb age of the inherited zircon is 636Ma, its $^{176}\text{Hf}/^{177}\text{Hf}$ ratio is 0.282411, its mean $\epsilon\text{Hf}(t)$ value is -7.7, and its corresponding T_{DM2} value is 2054Ma. All the Lu-Hf isotopic features obtained from inherited zircons indicate that the complexes are sourced partly by Late Paleoproterozoic to Early Mesoproterozoic continental crust and depleted mantle, with a minute quantity coming from the Archeozoic lower crust.

4.3 Whole-rock major, trace and rare earth element data

33 granitic samples were collected from the six complexes for major, trace and rare earth element (REE) analysis (Table 3 in Appendix C). As seen in the QAP diagram (Fig. 6) (Steckeseisen, 1976), granitic rocks from the Lat Boua, Kham and Laosang complexes fall into the monzogranite field. Granites from the Phon Thong and Na The complexes, as well as four samples from the Luu Complex, fall into the granodiorite field. Two samples from the Luu Complex fall into the tonalite field. All the samples have similar SiO_2 , $\text{Na}_2\text{O}+\text{K}_2\text{O}$ and Al_2O_3 contents, but their $\text{K}_2\text{O}/\text{Na}_2\text{O}$ ratios and aluminium indices (A/CNK) vary in different complexes (Table 4). Thus, in the K_2O vs. SiO_2 and A/NK vs. A/CNK diagrams (Fig.7) (Peccerillo and Taylor, 1976;

1 Middlemost, 1985; Maniar and Piccoli, 1989), samples from the Lat Boua, Kham, Na
2
3 The and Laosang complexes all fall into the peraluminous high-K calcalkaline field,
4
5 but samples from the Phon Thong and Luu complexes fall into the meta-aluminous
6
7 calcalkaline or meta-aluminous low-K fields.
8
9

10
11 Granite samples from the six complexes display similar patterns in the chondrite
12
13 (Boynton, 1984) and primitive mantle (Sun and McDonough, 1989) normalized rare
14
15 earth and trace element plots. All rocks show enriched Light Rare Earth Element
16
17 (LREE) and flat Heavy Rare Earth Element (HREE) chondrite-normalized REE
18
19 patterns (Fig. 8a), with the LREE/HREE ratio between 6.38 and 8.06 in the Lat Boua
20
21 Complex, between 6.87 and 7.83 in the Kham Complex, between 6.25 and 10.37 in
22
23 the Phon Thong Complex, between 5.30 and 9.48 in the Luu Complex, between 3.05
24
25 and 4.76 in the Na The Complex, and between 7.89 and 9.97 in the Laosang Complex.
26
27
28 The La_N/Yb_N ratio ranges from 7.19 to 10.03 in the Lat Boua Complex, from 7.23 to
29
30 8.80 in the Kham Complex, from 5.94 to 11.87 in the Phon Thong Complex, from
31
32 5.09 to 10.67 in the Luu Complex, from 2.78 to 4.70 in the Na The Complex, and
33
34 from 7.73 to 15.07 in the Laosang Complex. Eu negative anomalies are observed,
35
36 with mean σ Eu ranging from 0.49 to 0.56. The rocks have similar patterns in the
37
38 chondrite (Boynton, 1984) and primitive mantle (Sun and McDonough, 1989)
39
40 normalized rare earth and trace element plots, marked by variable enrichments in Rb,
41
42 Ba, Th and Ce and depletions in Ta, Nb, Sr and Ti (Fig. 8b). Furthermore, the Sr
43
44 values from all the samples are ca. 100–330ppm, other than for LH-14, which is
45
46 89ppm, and LT-7 and LB-4, which are as low as 58.7ppm. Yb values are <2ppm. The
47
48
49
50
51
52
53
54
55
56
57
58
59
60
61
62
63
64
65

1 granite shows low content in Sr and Yb, indicating that the magmatic source of the
2
3 granite contained relics of plagioclase and garnet. The original rocks are plagioclase
4
5 and garnet high-pressure metamorphic rocks. Additionally, in the Th/Yb vs. Ta/Yb
6
7 and Hf-Rb-Ta tectonic classification diagrams (Fig. 9) (Pearce, 1984; Harris *et al.*,
8
9 and Hf-Rb-Ta tectonic classification diagrams (Fig. 9) (Pearce, 1984; Harris *et al.*,
10
11 1986), all the granitic rocks fall into the volcanic arc granite field, and are classified
12
13 as I-type granites in the (Na₂O+K₂O) vs. (Zr+Nb+Ce+Y) and the Th vs. Rb diagrams
14
15 (Fig. 10) (Whalen *et al.*, 1987; Chappell and White, 1992). Overall, the whole-rock
16
17 major, trace and rare earth element characteristics of the 33 granites from the six
18
19 complexes are typical of I-type volcanic arc granites.
20
21
22
23
24
25
26
27

28 **5. Discussion**

29 **5.1 Crustal characteristics of the Indochina Block**

30
31
32
33
34 According to zircon U-Pb ages from northern Laos (Section 4.1), the Indochina
35
36 Block experienced two periods of magmatic activity from the Early Paleozoic to the
37
38 Early Mesozoic. One lasted from 402.5Ma to 435.1Ma, and the second from 234.3Ma
39
40 to 256.4Ma. Additionally, some inherited zircon cores disclose the occurrence of
41
42 magmatic from the Early Paleozoic to the Late Paleoproterozoic. Inherited zircon
43
44 grains from the same Indochina block in Malaysia and the Kontum Massif also
45
46 exhibit Proterozoic ages (800Ma, 1200Ma, 1350Ma, 1403Ma, 1600Ma, 1800Ma and
47
48 2600Ma) (Liew and McCulloch, 1985; Carter *et al.*, 2001; Nagy *et al.*, 2001).
49
50
51
52
53 Furthermore, detrital zircon ages from the Indochina Block also suggest that basement
54
55 metasedimentary rock protoliths were formed during the Meoproterozoic-Early
56
57
58
59
60
61
62
63
64
65

1 Paleozoic (Burrett *et al.*, 2014), which differs from the Archean basement age
2
3 (3.5–2.7Ga) obtained from central Vietnam, east of the Song Ma Suture (Lan *et al.*,
4
5
6 2001; Lan *et al.*, 2003).
7

8
9 Moreover, T_{MD2} ages of Late Permian to Early Triassic granites mainly range
10
11 from 1511 to 1621Ma in the Lat Boua Complex, 1670 to 1718Ma in the Kham
12
13 Complex, 1598Ma to 1613Ma in the Phon Thong Complex, 1735 to 1782Ma in the
14
15 Luu Complex and 1565 to 1584Ma in the Na The Complex. The T_{MD2} ages of some
16
17 spots fall within the 2500-2000Ma period, and only a few spots render modelled ages
18
19 older than 2500Ma. T_{MD2} ages of Early Paleozoic granite (Laosang Complex) are ca.
20
21 1702-1760Ma. The $\epsilon Hf(t)$ values of the 12 samples are almost all negative, with mean
22
23 $\epsilon Hf(t)$ values ranging from -3.4 to -8.2, indicating that these samples were sourced
24
25 principally by re-melted crust. Only a few spots have positive $\epsilon Hf(t)$ values,
26
27
28
29
30
31
32
33
34 indicating a depleted mantle source.
35

36
37 Zircon inheritance ages and T_{MD2} ages suggest that the main crust of the
38
39 Indochina Block was formed in the Late Paleoproterozoic to Early Mesoproterozoic,
40
41
42 and that the role of Archean rocks in the crustal evolution of the Indochina Block was
43
44 limited. This conclusion is similar to observations from the Kontum Massif (Carter *et*
45
46 *al.*, 2001; Nagy *et al.*, 2001) and in the East Coast Province batholiths of the
47
48 Malaysian Peninsula (Liew and McCulloch, 1985), located in the southwestern part of
49
50 the Indochina Block (Metcalf, 2000). The ages are much younger than those
51
52
53 obtained in the Cavin Complex of northern Vietnam, which is Archean (Lan *et al.*,
54
55
56 2001). The differences in crustal evolution between the Indochina Block and the
57
58
59
60
61
62
63
64
65

1 block east of the Song Ma Suture further confirm that the boundary between
2
3 Indochina and South China is the Song Ma Suture (Lepvrier *et al.*, 2004; Liu *et al.*,
4
5 2012; Faure *et al.*, 2014), not the Song Da or Song Chay sutures, as once assumed.
6
7
8
9

10 11 **5.2 A single Qamdo-Simao-Indochina block** 12

13
14 Overall, the characteristic patterns exhibited by whole-rock major, trace and rare
15
16 earth element data from the six plutons are typical of I-type volcanic arc granites
17
18 (Section 4.3; Figs. 6-10). This result is similar to data from the Dien Bien granite
19
20 massif west of the Song Ma Suture (Lan *et al.*, 2001; Liu *et al.*, 2012; Roger *et al.*,
21
22 2014). The granites located at the junction of the Dien Bien Phu and Song Ma sutures,
23
24 and once attributed to the Sibumasu-Simao Block, clearly subducted eastward under
25
26 the Indochina Block along the Dien Bien Phu Suture. Sengor and Hsu (1984) named
27
28 the Dien Bien Phu Suture the “Dien Bien Phu arm of the Paleo-Tethys”. Leloup *et al.*
29
30 (1995) correlated the Dien Bien Suture with the Jinsha River Suture as fault markers
31
32 of the Ailaoshan-Red River Fault, calculating that Indochina extruded ca. 500-700km
33
34 along the Ailaoshan left-lateral strike slip fault during 35-22Ma. However, recent
35
36 geochronological studies have disclosed that the initiation time of the Dien Bien Phu
37
38 Fault was after 228Ma (Lin *et al.*, 2009; Roger *et al.*, 2014); the fault thus mismatches
39
40 the volcanic arc I-type granites described in this paper. Furthermore, structural studies
41
42 (DGM, 1991; Lepvrier *et al.*, 1997; Lin *et al.*, 2009; Faure *et al.*, 2014; Roger *et al.*,
43
44 2014) show that the Song Ma Suture is right-laterally offset ca. 30-40km by the Dien
45
46 Bien Phu Fault; the strata and fold axes have also bent eastward, but the primary
47
48
49
50
51
52
53
54
55
56
57
58
59
60
61
62
63
64
65

1 structure of the Truong Son Belt has not been significantly altered. So, the Dien Bien
2
3 Phu Fault does not present a suture branch separating Qamdo-Simao from the
4
5 Indochina Block. Thus, the Nan Suture should connect northward with the Jinghong
6
7 Suture (Sone and Metcalfe, 2008; Faure *et al.*, 2014), and the
8
9 Qamdo-Simao-Indochina Block should be a united block (Fig. 11).
10
11
12
13

14 The similarity of the characteristics of the Qamdo-Simao and Indochina blocks
15
16 when treated as a united block can be proven using other evidence. First, although
17
18 Lepvrier *et al.* (1997, 2004) suggested that the Indochina Block subducted eastward
19
20 under South China during the Late Permian-Early Triassic, increasing quantities of
21
22 structural, geochronological and geochemical data confirm that the geometry of the
23
24 block convergence between Indochina and South China was a westward subduction of
25
26 South China under Indochina (Liu *et al.*, 2012; Faure *et al.*, 2014; this paper). The
27
28 same is true for South China subducting westward under the Qamdo-Simao Block.
29
30 The precise timing of the two block convergences has been corrected from 220Ma
31
32 (Rb-Sr age, Wang *et al.*, 2000) to 270–240Ma (Jian *et al.*, 2008, 2009; Lai *et al.*,
33
34 2014), almost the same age as we obtained in this paper. Secondly, the 440-400Ma
35
36 granite complexes that were found along the Jinsha River Suture in China (*e.g.* Jian *et*
37
38 *al.*, 2009), have also been found along the Song Ma Suture (this paper) and along the
39
40 Kontum Massif in Vietnam (*e.g.* Carter *et al.*, 2001; Nagy *et al.*, 2001; Sanematsu *et*
41
42 *al.*, 2011). There is no magmatic event either in the Qamdo-Simao Block or in the
43
44 Indochina Block from 400Ma to 280Ma. Thus the Qamdo-Simao Block and the
45
46 Indochina Block experienced similar magmatic events from the Early Paleozoic to the
47
48
49
50
51
52
53
54
55
56
57
58
59
60
61
62
63
64
65

1 Early Mesozoic. Instead, the early Paleozoic magmatic event before the Indosinian
2
3 magmatic event in Sibumasu-Bao Shan-South Qiangtang block occurred around
4
5 500-470Ma (*e.g.* Lin *et al.*, 2013; Dong *et al.*, 2013; Hu *et al.*, 2015), about 100-60Ma
6
7 earlier than that in the Qamdo-Simao-Indochina block. Further, evidence of the
8
9 existence of the same Gigantopteris flora and warm-water fauna in the Indochina and
10
11 Qamdo-Simao blocks proves that they were once rifted and drifted northward from
12
13 Gondwana in the Early Devonian (Metcalf, 1996, 1999). Lastly, as deduced from
14
15 ϵNd and T_{MD2} ages, the principal period of crust formation in the Qamdo Block was
16
17 ca. 1.4-1.7Ga (*e.g.* Zhai *et al.*, 2012; Zhang *et al.*, 2014), similar to that of the
18
19 Indochina Block.
20
21
22
23
24
25
26
27
28
29
30

31 **5.3 The Jinsha River Suture-Song Ma Suture-Kontum Massif as the boundary** 32 33 **between the Qamdo-Simao-Indochina and South China blocks** 34 35

36 The Late Permian-Early Triassic I-type granites detailed in this paper belong to
37
38 the Truong Son Belt, thus corroborating the tectonic model of the South China Block
39
40 subducting westward under the Indochina Block (Liu *et al.*, 2012; Faure *et al.*, 2014).
41
42 In interpreting the relation between the Song Ma and Song Chay sutures in northern
43
44 Vietnam, Faure *et al.* (2014) suggested that these two northern Vietnam belts are parts
45
46 of a single orogen dismembered by Cenozoic wrenching along the Red River Fault.
47
48 There are several reasons for disagreeing with this hypothesis.
49
50
51
52
53
54

55 First, structural studies (Lepvrier *et al.*, 1997, 2004, 2008; Tran *et al.*, 2014) show
56
57 an E-W striking shifting to a N-S striking along the Tam Ky-Phuoc Son Suture in the
58
59
60
61
62
63
64
65

1 southern part of the Truong Son Belt, and north of the Kontum Massif. Southward,
2
3 the Tam Ky-Phuoc Son suture connects with the Poko Suture west of the Kontum
4
5 Massif. Geochronological magmatism (*e.g.* Carter *et al.*, 2001; Nagy *et al.*, 2001; Lan
6
7 *et al.*, 2000; Owada *et al.*, 2007; Sanematsu *et al.*, 2011) and metamorphism (*e.g.* Lan
8
9 *et al.*, 2003; Osanai *et al.*, 2001, 2004; Nakano *et al.*, 2007) relating to the Poko suture
10
11 also give ages between 260Ma and 240Ma. Lepvrier *et al.* (2008) even suggest that
12
13 the Kontum Massif subducted westward under the Indochina Block, with the time and
14
15 manner the same as for the two blocks along the Song Ma Suture (this paper; Liu *et*
16
17 *al.*, 2012; Faure *et al.*, 2014). Thus, if the Song Ma Suture is offset from the Jinsha
18
19 -Song Chay Suture, the role of the Kontum Massif in the convergence of Indochina
20
21 and South China *vis-à-vis* the Poko Suture is difficult to interpret.
22
23
24
25
26
27
28
29
30

31 Second, if the Song Ma Suture Zone is taken as forming the northern segment of
32
33 the Song Chay Suture, there would be no system of tectonic units related to the
34
35 Indochina orogenic zone around the Song Chay Suture. For example, no volcanic arc
36
37 belt exists on either side of the Song Chay Suture; granites southwest of the Song
38
39 Chay Suture are A-type granite with positive Nd(t) values (Pham *et al.*, 2013), and are
40
41 thus related to the Song Da Rift.
42
43
44
45
46

47 Third, in the Indochina Block, there is no other continental-scale ductile shear
48
49 zone that, coupled with the Ailaoshan-Red River Fault, could produce the
50
51 documented Early Miocene Truong Son Belt extrusion. For example, within the
52
53 Indochina Block, the Dien Bien Phu Fault forms the western boundary of the Truong
54
55 Son Belt, but geochronological and structural studies show that it was a right-lateral
56
57
58
59
60
61
62
63
64
65

1 strike slip fault after 228Ma, with 30-40km offset ; the fault, as the southernmost part
2
3 of the Xianshuihe fault system, was reactive from ca. 5Ma to the present, with a
4
5 left-lateral offset <10km (*e.g.* Wang *et al.*, 1998; Zuchiewicz *et al.*, 2004; Koszowska
6
7
8
9 *et al.*, 2007; Lin *et al.*, 2009; Roger *et al.*, 2014).

10
11 We therefore propose that the Jinsha River Suture, the Song Ma Suture and the
12
13 Kontum Massif form the boundary between the Indochina and South China blocks.
14
15
16

20 **5.4 The Emeishan Plume: the dynamics of a Permo-Triassic block convergence**

21
22 Southeast Asia is a composite landmass of Gondwana-derived continental blocks.
23
24 Having been detached from the northeastern margin of Gondwana, they progressively
25
26 assembled with each other and accreted to form a proto-Asia. A major part of this
27
28 evolution took place from the Mid Paleozoic to the Early Mesozoic. Several episodes
29
30 of rifting and northward drifting occurred, followed by subduction and subsequent
31
32 narrowing and closure of different branches of the Paleotethyan Ocean (*e.g.*
33
34 Hutchison, 1989; Sengor, 1979; Sengor and Hsu, 1984; Metcalfe, 1986, 1999, 2002;
35
36 Lepvrier *et al.*, 1997, 2004, 2008). Without doubt, the closure of the Paleotethyan
37
38 Ocean and the opening of the Mesotethyan Ocean provided the main dynamics for the
39
40 convergence of the Sibumasu, Qamdo-Simao-Indochina and South China blocks.
41
42 Against this background, we would also suggest that the Emeishan Plume contributed
43
44 to the convergence of the Qamdo-Simao-Indochina and South China blocks.
45
46
47
48
49
50
51
52
53

54
55 The Emeishan basalts, also known as the Emeishan large igneous province
56
57 (ELIP), outcrop principally in the Chinese provinces of Sichuan, Yunnan and
58
59
60

1 Guizhou and the Song Da region of northern Vietnam. The ELIP is composed mainly
2
3 of flood basalts and mafic-ultramafic intrusions. The volcanic sequence ranges in
4
5 thickness from several hundred meters in the east to nearly 5km in the west (Chung
6
7 and Jahn, 1995; Song *et al.*, 2001; Xu *et al.*, 2001; Xiao *et al.*, 2004). The lavas
8
9 include picrites, tholeiites and basaltic andesites, all of which are believed to have
10
11 formed from an upwelling mantle plume (Chung and Jahn, 1995; Xu *et al.*, 2001;
12
13 Zhou *et al.*, 2006). Recent research has found that Late Permian A-type granite is
14
15 related to the Emeishan Plume in the Panzhihua and Dali rifts in the Sichuan-Yunnan
16
17 area (Shellnutt *et al.*, 2007, 2009), similar to a study of the Song Da rift (Pham *et al.*,
18
19 2013). Permian flood basalts and associated mafic-ultramafic intrusions form a
20
21 narrow (≤ 20 km), NW-trending belt >350 km long in the Jinping-Song Da Rift. The
22
23 belt is bounded by the Ailaoshan-Red River Fault Zone to the northeast and the
24
25 Jinsha-Song Ma Suture to the southwest (Wang *et al.*, 2007). South of this, there is no
26
27 report of Emeishan basalts outcropping in the Kontum Massif, but a NW-SE striking
28
29 normal shear zone has developed in the Ngoc Linh and Kannack complexes, which is
30
31 composed of HT to UHT metamorphic rocks (Osanai *et al.*, 2004; Lepvrier *et al.*,
32
33 2008). Both the Ngoc Linh and the Kannak complexes are locally intruded by granitic
34
35 rocks, with fine-grained gabbro enclaves; the igneous activity and HT to UHT
36
37 metamorphism coincide with each other at 250Ma to 260Ma. An upwelling mantle
38
39 plume would explain the formation of the syn-tectonic magmatism with the HT-UHT
40
41 metamorphism (Osanai *et al.*, 2001, 2004; Owada *et al.*, 2007). The plume related to
42
43 the Emeishan Plume thus appears to represent a particular tectonic feature at the
44
45
46
47
48
49
50
51
52
53
54
55
56
57
58
59
60

1 western boundary of the South China Block.
2

3 I-type volcanic arc granites in the Late Permian-Early Triassic can be treated as
4 an index of the subduction between the Sibumasu, Indochina and South China blocks
5 during the Paleotethyan Ocean closure (Carter *et al.*, 2001; Lepvrier *et al.*, 2004, 2008;
6 Liu *et al.*, 2012). Subsequently, S-type granites with 220Ma to 200Ma ages, as well as
7 I-type granites of Late Mesozoic age, developed at the western boundary of the
8 Sibumasu Block (*e.g.* Charusiri, 1993; Searle *et al.*, 2012), indicating compressional
9 conditions during the Mesozoic. In contrast, A-type granites developed after 200Ma
10 in the South China Block. It has been suggested that these magmas were generated as
11 a consequence of intraplate extension in the western part of the South China Block
12 (*e.g.* Chung *et al.*, 1997; Lan *et al.*, 2000; Maluski *et al.*, 2001). The different stresses
13 prevalent in the South China Block *vis-à-vis* the Sibumasu Block could be attributed
14 to the dynamic conditions produced by the Emeishan Plume in the mantle after
15 260Ma. We therefore propose that the Emeishan Plume formed part of the dynamic
16 driving Permo-Triassic block convergence and subsequent extension into the South
17 China Block (Fig. 12).
18
19
20
21
22
23
24
25
26
27
28
29
30
31
32
33
34
35
36
37
38
39
40
41
42
43
44
45
46

47 **6. Conclusions**

48 33 samples from six granite complexes along the road from Phonsavan to Sam
49 Neua in northern Laos were selected for zircon U-Pb age, Lu-Hf ratio and whole-rock
50 major, trace and rare earth element analysis. Geochronological and geochemical data
51 from these samples can be summarized as follows:
52
53
54
55
56
57
58
59
60

1 1) The zircon U-Pb ages of 600 spots from 16 samples taken from five granite
2
3 complexes range from 234Ma to 256Ma. 234-256Ma magmatic arc granites mismatch
4
5 the initiation time of the Dien Bien Phu fault. The existence of the Dien Bien Phu
6
7 Suture can therefore be repudiated. This evidence further suggests the existence of a
8
9 united Qamdo-Simao-Indochina Block.
10
11
12

13
14 2) The $\epsilon_{\text{Hf}}(t)$ values of zircon Lu-Hf data from a total of 201 spots from 20
15
16 samples are generally negative, with corresponding T_{DM2} ages dated to the Late
17
18 Paleoproterozoic. Zircon inheritance ages and T_{MD2} ages suggest that the formation of
19
20 the main crust of the Indochina Block was during the Late Paleoproterozoic; these
21
22 ages are much younger than the Archean ages obtained in the Cavinh Complex of
23
24 northern Vietnam east of the Song Ma Suture. Thus, the different crustal evolutions of
25
26 the Indochina Block and the block east of the Song Ma Suture further confirm that the
27
28 boundary between Indochina and South China is the Song Ma Suture rather than the
29
30 Song Da or Song Chay sutures.
31
32
33
34
35
36
37
38

39 3) Major, trace and rare earth element data from the granitic rocks of six
40
41 complexes indicate mainly peraluminous high-K calcalkaline granite. The Indochina
42
43 granite samples have similar patterns in their chondrite and primitive mantle
44
45 normalized rare earth and trace element plots, marked by variable enrichments in Rb,
46
47 Ba, Th and Ce and depletions in Ta, Nb, Sr and Ti, typical of I-type volcanic arc
48
49 granites. These granites, together with other tectonic units of the Song Ma Suture,
50
51 suggest a westward subduction of the South China Block beneath the
52
53 Qamdo-Simao-Indochina Block.
54
55
56
57
58
59
60

1 4) 440-404Ma and 234-256Ma I-type granites suggest that the boundary between
2
3 Indochina and South China should be the Jinsha River Suture–Song Ma
4
5 Suture–Kontum Massif, rather than the Jinsha-Song Chay Suture.
6
7

8
9 5) Both the Emeishan basalt and granite complexes form part of the tectonic
10
11 units of the South China Block subducting westward under the
12
13 Qamdo-Simao-Indochina Block. The plume beneath the Emeishan basalt also
14
15 contributes to the convergence of the two blocks following the opening of the
16
17 Mesotethyan Ocean.
18
19
20
21
22
23
24

25 **Acknowledgments**

26
27
28 This research was funded jointly by the Basic Science Research Fund of the
29
30 Institute of Geomechanics, CAGS (Grant No. DZLXJK201410, DZLXJK201406);
31
32 the China Geological Survey (Grant Nos. 12120115000701, 12120114002101); and
33
34 the National Natural Science Foundation of China (Grant No. 41172192). We would
35
36 like to thank Profs. Metcalfe Ian, Morley Chris, Chung Sunlin and two anonymous
37
38 reviewers for their constructive comments which greatly improved the quality of the
39
40 draft. Thanks also give Drs. Dong Yunpeng and Kwon Sanghoon for their work on
41
42 the manuscript.
43
44
45
46
47
48
49
50
51
52

53 **References:**

54
55 Andersen, T., 2002. Correction of common lead in U–Pb analyses that do not report
56
57 204Pb. *Chemical Geology* 192, 59–79.
58
59
60
61
62
63
64
65

1 Barr, S.M. and MacDonald, A.S., 1987. Nan River suture zone, northern
2
3 Thailand. *Geology* 15, 907–910.
4

5
6 Barr, S.M., MacDonald, A.S., Dunning, G.R., Ounchanum, P., Yaowanoyothin, W.,
7
8 2000. Petrochemistry, U–Pb (zircon) age, and palaeotectonic setting of the Lampang
9
10 volcanic belt, northern Thailand. *Journal of the Geological Society of London* 157,
11
12 553-563.
13
14

15
16
17 Beckinsale, R.D., Suensilpong, S., Nakapadungrat, S., 1979. Geochronology and
18
19 geochemistry of granite magmatism in Thailand in relation to plate tectonic models.
20
21 *Journal of the Geological Society of London* 136, 529-540.
22
23

24
25 Blichert-Toft, J., Albarède, F., 1997. The Lu–Hf geochemistry of chondrites and the
26
27 evolution of the mantle–crust system. *Earth and Planetary Science Letters* 148,
28
29 243–258.
30
31

32
33 Boynton, W. V. 1984. *Cosmochemistry of the Rare Earth Elements: Meteorite Studies*.
34
35 Elsevier Science Publishing Company: Amsterdam.
36
37

38
39 Burrett, C., Khin Zaw, Meffre, S., Lai, C.K., Khositantont, S., Chaodumrong, P.,
40
41 Udchachon, M., Ekins, S., Halpin, J., 2014. The configuration of Greater Gondwana
42
43 — evidence from LA ICPMS, U–Pb geochronology of detrital zircons from the
44
45 Palaeozoic and Mesozoic of Southeast Asia and China. *Gondwana Research* 26 (1),
46
47 31–51.
48
49

50
51
52 Carter, A., Clift, P.D., 2008. Was the Indosinian orogeny a Triassic mountain building
53
54 or a thermotectonic reactivation event? *Comptes Rendus Geoscience* 340, 83–93.
55
56

57
58 Carter, A., Roques, D., Bristow, C., Kinny, P., 2001. *Understanding Mesozoic*
59
60

1 accretion in Southeast Asia: significance of Triassic thermotectonism (Indochina
2
3 Orogeny) in Vietnam. *Geology* 29 (3), 211-214.
4

5
6 Chappell, B. W., White, A. J. R. 1992. I- and S-type granites in the Lachlan Fold Belt.
7
8
9 Transactions of the Royal Society of Edinburgh: Earth sciences 83(1–2), 1–26.
10

11
12 Charusiri, P., Clark, A.H., Farrar, E., Archibald, D., Charusiri, B., 1993. Granites
13
14 belts in Thailand: evidence from the $^{40}\text{Ar}/^{39}\text{Ar}$ geochronological and geological
15
16 syntheses. *Journal of Southeast Asian Earth Sciences* 8, 127-136.
17
18

19
20 Chung, S.L., Jahn, B.M., 1995. Plume–lithosphere interaction in generation of the
21
22 Emeishan flood basalts at the Permian–Triassic boundary. *Geology* 23, 889–892.
23
24

25
26 Chung, S., Lee, T., Lo, C., Wang, P., Chen, C., Yem, N., Tran Trong Hoa, Wu, G.,
27
28 1997. Intraplate extension prior to continental extrusion along the Ailao Shan–Red
29
30 River shear zone. *Geology* 25(4), 311-314.
31
32

33
34 Department of Geology and Mine, Lao P. D. R. (DGM), 1991. Geological and
35
36 Mineral Occurrence Map. 1:1000000 scale. British Geological Survey and
37
38 Department of Geology and Mines.
39
40

41
42 Department of Geological and Minerals of Vietnam (DGMV), 2005. Geology and
43
44 mineral resources map of Phong Saly-Dien Bien Phu Sheet, scale 1: 200000, with the
45
46 explanatory note, Hanoi.
47
48

49
50 Dong, M., Dong, G., Mo, X., Santosh, M., Zhu, D., Yu, J., Nie, F., Hu, Z., 2013.
51
52 Geochemistry, zircon U–Pb geochronology and Hf isotopes of granites in the Baoshan
53
54 Block, Western Yunnan: Implications for Early Paleozoic evolution along the
55
56 Gondwana margin. *Lithos* 179, 36–47.
57
58
59
60

1 Ferrari, O.M., Hochard, C., Stampfli, G.M., 2008. An alternative plate tectonic model
2
3 for the Palaeozoic-Early Mesozoic Palaeotethyan evolution of Southeast Asia
4
5 (Northern Thailand–Burma). *Tectonophysics* 451, 346-365.
6
7

8
9 Faure, M., Lepvrier, C., Nguyen, V., Vu, T., Lin, W. and Chen, Z., 2014, The South
10
11 China block-Indochina collision: Where, when, and how? *Journal of Southeast Asian*
12
13 *Earth Sciences* 79, 260-274.
14
15

16
17 Gardiner, N. J., Searle, M.P., Morley, C.K., Whitehouse, M.P., Spencer, C. J., Robb,
18
19 L.J., 2015. The closure of Paleo-Tethys in Eastern Myanmar and Northern Thailand:
20
21 new insights from zircon U-Pb and Hf isotope data. *Gondwana Research*,
22
23 <http://dx.doi.org/10.1016/j.gr.2015.03.001>.
24
25
26

27
28 Griffin, W.L., Wang, X., Jackson, S.E., Pearson, N.J., O'Reilly, S.Y., Xu, X., Zhou,
29
30 X., 2002. Zircon chemistry and magmamixing, SE China: in-situ analysis of Hf
31
32 isotopes, Tonglu and Pingtan igneous complexes. *Lithos* 61, 237–269
33
34
35

36
37 Harris N.B.W., Pearce J.A., Tindle A.G. 1986. Geochemical characteristics of
38
39 collision-zone magmatism. In: Coward M.P., Rles A.C. (Eds.). *Collision Tectonics*,
40
41 vol.19. Geological Society, London, Special Publications, pp.67-81.
42
43

44
45 Hu, P., Zhai, Q., Jahn, B., Wang, J., Lee, H., Tang, S., 2015. Early Ordovician
46
47 granites from the South Qiangtang terrane, northern Tibet: Implications for the early
48
49 Paleozoic tectonic evolution along the Gondwanan proto-Tethyan margin. *Lithos*,
50
51 <http://dx.doi.org/10.1016/j.lithos.2014.12.020>
52
53
54

55
56 Hutchison, C.S. 1975. Ophiolite in Southeast Asia. *Geological Society of America*
57
58 *Bulletin*, 86, 797–806.
59
60

1 Hutchison, C.S. 1989. 1989. South-East Asian Oil, Gas, Coal and Mineral Deposits.
2
3 Oxford Monographs on Geology and Geophysics, 13.
4

5
6 Jackson, S. E., Pearson, N. J., Griffin, W. L., Belousova, E. A. 2004. The application
7
8 of laser ablation-inductively coupled plasma-mass spectrometry to in situ U–Pb zircon
9
10 geochronology. Chemical Geology 211(1–2), 47–69. DOI:
11
12 10.1016/j.chemgeo.2004.06.017.
13
14

15
16
17 Janvier, P., Tong-Dzuy, T., Ta Hoa, P., Doan Nhat, T., 1997. The Devonian
18
19 vertebrates (Placodermi, Sarcopterygii) from Central Vietnam and their bearing on the
20
21 Devonian paleogeography of Southeast Asia. Journal of Asian Earth Sciences 15,
22
23 393–406.
24
25

26
27
28 Jian, P., Liu, D.Y., Sun, X.M., 2008. SHRIMP dating of the Permo-Carboniferous
29
30 Jinshajiang ophiolite, southwestern China: Geochronological constraints for the
31
32 evolution of Paleo-Tethys. Journal of Asian Earth Sciences 32, 371–384.
33
34

35
36 Jian, P., Liu, D.Y., Kröner, A., Zhang, Q., Wang, Y.Z., Sun, X.M., Zhang, W., 2009.
37
38 Devonian to Permian plate tectonic cycle of the Paleo-Tethys Orogen in southwest
39
40 China (II): Insights from zircon ages of ophiolites, arc/back-arc assemblages and
41
42 withinplate igneous rocks and generation of the Emeishan CFB province. Lithos 113,
43
44 767–784.
45
46
47

48
49 Koszowska, E., Wolska, A., Zuchiewicz, W., Nguyen, Q., Pe' cskay, Z., 2007.
50
51 Crustal contamination of Late Neogene basalts in the Dien Bien Phu Basin, NW
52
53 Vietnam: Some insights from petrological and geochronological studies. Journal of
54
55 Asian Earth Sciences 29, 1–17.
56
57
58
59
60

1 Lai, C.K., Meffre, S., Crawford, A.J., Khin Zaw, Xue, C.D., Halpin, J., 2014. The
2
3 Western Ailaoshan volcanic belts and their SE Asia connection: a new tectonic model
4
5
6 for the Eastern Indochina Block. *Gondwana Research* 26 (1), 52–74.
7

8
9 Lan, C.Y., Chung, S.L., Shen, J.J., Lo, C.H., Wang, P.L., Tran Trong-Hoa, Hoang Huu
10
11 Thanh, Mertzman, S.A., 2000. Geochemical and Sr–Nd isotopic characteristics of
12
13 granitic rocks from northern Vietnam. *Journal of Asian Earth Sciences*, 267-280.
14

15
16
17 Lan, C.Y., Chung, S.L., Lo, C.H., Lee, T.Y., Wang, P.L., Li, H., Toan, D.V., 2001.
18
19
20 First evidence for Archean continental crust in northern Vietnam and its implications
21
22 for crustal and tectonic evolution in southeast Asia. *Geology* 29 (3), 219–222.
23

24
25
26 Lan, C., Chung, S., Trinh Van Long, Lo, C., Lee, T., Mertzman, S., Shen, J., 2003.
27
28
29 Geochemical and Sr–Nd isotopic constraints from the Kontum massif, central
30
31 Vietnam on the crustal evolution of the Indochina block. *Precambrian Research* 122,
32
33 7-27.
34

35
36
37 Leloup, P.H., Lacassin, R., Tapponnier, R., Zhong, D., Lui, X., Zhang, L., Ji, S., Trinh,
38
39 P. T., 1995. The Ailao Shan–Red River shear zone (Yunnan, China), Tertiary
40
41 transform boundary of Indochina. *Tectonophysics* 251, 3-84.
42

43
44
45 Lepvrier, C., Maluski, H., Nguyen Van Vuong, Roques, D., Axente, V., Rangin, G.,
46
47
48 1997. Indochina NW-trending shear zones within the Truong Son belt (Vietnam).
49
50
51 *Tectonophysics* 283, 105-127.
52

53
54
55 Lepvrier, C., Maluski, H., Van Tich, V., Leyreloup, A., Truong Thi, P., Van Vuong,
56
57
58 N., 2004. The Early Triassic Indochina orogeny in Vietnam (Truong Son Belt and
59
60
61 Kontum Massif); implications for the geodynamic evolution of Indochina.
62

1 Tectonophysics 393, 87-118.

2
3 Lepvrier, C., Vuong, Nguyen Van, Maluski, H., Thi, Phan Truong, Tich, Vu Van,
4
5
6 2008. Indosinian tectonics in Vietnam. *Comptes Rendus Geoscience* 340, 94–111.

7
8
9 Lepvrier, C., Faure, M., Van Vuong, Nguyen, Van Vu, Tich, Lin, W., Thang, Ta
10
11 Trong, Phuong, Ta Hoa, 2011. North-directed Triassic nappes in Northeastern
12
13 Vietnam (East Bac Bo). *Journal of Asian Earth Sciences* 41, 56–68.

14
15
16
17 Liew, T.C. and McCulloch, M.T., 1985. Genesis of granitoid batholiths of Peninsular
18
19 Malaysia and implications for models of crustal evolution: evidence from Nd–Sr
20
21 isotopic and U–Pb zircon study. *Geochimica et Cosmochimica Acta* 49, 587-600.

22
23
24
25 Lin, T., Lo, C., Chung, S., Wang, P., Yeh, M., Lee, T., Lan, C., Nguyen, V., Tran, T.,
26
27 2009. Jurassic Dextral Movement along the Dien Bien Phu Fault, NW Vietnam:
28
29 Constraints from $^{40}\text{Ar}/^{39}\text{Ar}$ Geochronology. *The Journal of Geology* 117, 192–199.

30
31
32
33 Lin, Y., Yeh, M., Lee, T., Chung, S., Lizuka, Y., Charusiri, P., 2013. First evidence of
34
35 the Cambrian basement in Upper Peninsula of Thailand and its implication for crustal
36
37 and tectonic evolution of the Sibumasu terrane. *Gondwana Research* 24, 1031–1037.

38
39
40
41 Liu, J., Tran, M., Tang, Y., Nguyen, Q.L., Tran, T.H., Wu, W., Chen, J., Zhang, Z.,
42
43 Zhao, Z., 2012. Permo-Triassic granitoids in the northern part of the Truong Son belt,
44
45 NW Vietnam: geochronology, geochemistry and tectonic implications. *Gondwana*
46
47
48
49
50
51
52
53
54
55
56
57
58
59
60
61
62
63
64
65
66
67
68
69
70
71
72
73
74
75
76
77
78
79
80
81
82
83
84
85
86
87
88
89
90
91
92
93
94
95
96
97
98
99
100
101
102
103
104
105
106
107
108
109
110
111
112
113
114
115
116
117
118
119
120
121
122
123
124
125
126
127
128
129
130
131
132
133
134
135
136
137
138
139
140
141
142
143
144
145
146
147
148
149
150
151
152
153
154
155
156
157
158
159
160
161
162
163
164
165
166
167
168
169
170
171
172
173
174
175
176
177
178
179
180
181
182
183
184
185
186
187
188
189
190
191
192
193
194
195
196
197
198
199
200
201
202
203
204
205
206
207
208
209
210
211
212
213
214
215
216
217
218
219
220
221
222
223
224
225
226
227
228
229
230
231
232
233
234
235
236
237
238
239
240
241
242
243
244
245
246
247
248
249
250
251
252
253
254
255
256
257
258
259
260
261
262
263
264
265
266
267
268
269
270
271
272
273
274
275
276
277
278
279
280
281
282
283
284
285
286
287
288
289
290
291
292
293
294
295
296
297
298
299
300
301
302
303
304
305
306
307
308
309
310
311
312
313
314
315
316
317
318
319
320
321
322
323
324
325
326
327
328
329
330
331
332
333
334
335
336
337
338
339
340
341
342
343
344
345
346
347
348
349
350
351
352
353
354
355
356
357
358
359
360
361
362
363
364
365
366
367
368
369
370
371
372
373
374
375
376
377
378
379
380
381
382
383
384
385
386
387
388
389
390
391
392
393
394
395
396
397
398
399
400
401
402
403
404
405
406
407
408
409
410
411
412
413
414
415
416
417
418
419
420
421
422
423
424
425
426
427
428
429
430
431
432
433
434
435
436
437
438
439
440
441
442
443
444
445
446
447
448
449
450
451
452
453
454
455
456
457
458
459
460
461
462
463
464
465
466
467
468
469
470
471
472
473
474
475
476
477
478
479
480
481
482
483
484
485
486
487
488
489
490
491
492
493
494
495
496
497
498
499
500
501
502
503
504
505
506
507
508
509
510
511
512
513
514
515
516
517
518
519
520
521
522
523
524
525
526
527
528
529
530
531
532
533
534
535
536
537
538
539
540
541
542
543
544
545
546
547
548
549
550
551
552
553
554
555
556
557
558
559
560
561
562
563
564
565
566
567
568
569
570
571
572
573
574
575
576
577
578
579
580
581
582
583
584
585
586
587
588
589
590
591
592
593
594
595
596
597
598
599
600
601
602
603
604
605
606
607
608
609
610
611
612
613
614
615
616
617
618
619
620
621
622
623
624
625
626
627
628
629
630
631
632
633
634
635
636
637
638
639
640
641
642
643
644
645
646
647
648
649
650
651
652
653
654
655
656
657
658
659
660
661
662
663
664
665
666
667
668
669
670
671
672
673
674
675
676
677
678
679
680
681
682
683
684
685
686
687
688
689
690
691
692
693
694
695
696
697
698
699
700
701
702
703
704
705
706
707
708
709
710
711
712
713
714
715
716
717
718
719
720
721
722
723
724
725
726
727
728
729
730
731
732
733
734
735
736
737
738
739
740
741
742
743
744
745
746
747
748
749
750
751
752
753
754
755
756
757
758
759
760
761
762
763
764
765
766
767
768
769
770
771
772
773
774
775
776
777
778
779
780
781
782
783
784
785
786
787
788
789
790
791
792
793
794
795
796
797
798
799
800
801
802
803
804
805
806
807
808
809
810
811
812
813
814
815
816
817
818
819
820
821
822
823
824
825
826
827
828
829
830
831
832
833
834
835
836
837
838
839
840
841
842
843
844
845
846
847
848
849
850
851
852
853
854
855
856
857
858
859
860
861
862
863
864
865
866
867
868
869
870
871
872
873
874
875
876
877
878
879
880
881
882
883
884
885
886
887
888
889
890
891
892
893
894
895
896
897
898
899
900
901
902
903
904
905
906
907
908
909
910
911
912
913
914
915
916
917
918
919
920
921
922
923
924
925
926
927
928
929
930
931
932
933
934
935
936
937
938
939
940
941
942
943
944
945
946
947
948
949
950
951
952
953
954
955
956
957
958
959
960
961
962
963
964
965
966
967
968
969
970
971
972
973
974
975
976
977
978
979
980
981
982
983
984
985
986
987
988
989
990
991
992
993
994
995
996
997
998
999
1000

1 Ludwig, K. R. 2003. User's manual for Isoplot 3.00: a geochronological toolkit for
2
3 Microsoft Excel, Berkeley Geochronology Center Special Publication 4.
4

5
6 Maluski, H., Lévrier, C., Jolivet, L., Carter, A., Roques, D., Beyssac, O., Nguyen,
7
8 D.T., Ta, T.T., Avigad, D., 2001. Ar–Ar and fission track ages in the Song Chay
9
10 massif: early Triassic and Cenozoic tectonics in northern Vietnam. *Journal of Asian*
11
12 *Earth Sciences* 19, 233–248.
13

14
15
16 Maniar, P. D., Piccoli, P. M., 1989. Tectonic discrimination of granitoids. *Geological*
17
18 *Society of America Bulletin* 101, 635–643.
19

20
21
22 Metcalfe, I., 1996. Pre-Cretaceous evolution of SE Asian terranes. In: Hall, R.,
23
24 Blundell, D. (Eds.), *Tectonic evolution of Southeast Asia*. Geological Society of
25
26 London Special Publication 106, 97-122.
27

28
29
30 Metcalfe, L., 1999. Gondwana dispersion and Asian accretion: an overview. In:
31
32 Metcalfe, I. (Ed.), *Gondwana Dispersion and Asian Accretion. Final Results Volume*
33
34 *for IGCP Project 321*. Balkema, Rotterdam, pp. 9-28.
35

36
37
38 Metcalfe, I., 2002. Permian tectonic framework and paleogeography of SE Asia.
39
40 *Journal of Asian Earth Sciences* 20, 551-566.
41

42
43
44 Metcalfe, I., 2013. Gondwana dispersion and Asian accretion: tectonic and
45
46 palaeogeographic evolution of eastern Tethys. *Journal of Asian Earth Sciences* 66,
47
48 1–33.
49

50
51
52 Middlemost E A K. 1985. *Magmas and Magmatic Rocks*. London: Longman, 1~266.
53

54
55
56 Nagy, E.A., Maluski, H., Lévrier, Q., Scharer, U., Thi, P.T., Leyreloup, A., 2001.
57
58 *Geodynamic significance of the Kontum massif in Central Vietnam: Composite*
59

1 40Ar/39Ar and U/Pb ages from Paleozoic to Triassic. *Journal of Geology* 109,
2
3 755-770.

4
5
6 Nakano, N., Osanai, Y., Owada, N., Hayasaka, Y., Tran Ngoc Nam, 2007.
7
8 Permo-Triassic Barrovian metamorphism in the Kontum massif, central Vietnam:
9
10 constraints on continental collision tectonics in Southeast Asia. *Gondwana Research*
11
12 12, 438-453.

13
14
15
16
17 Osanai, Y., Owada, M., Tsunogae, T., Toyoshima, T., Hokada, T., Long, T.V., Sajeev,
18
19 K. and Nakano, N., 2001. Ultrahigh-temperature polytic granulites from Kontum
20
21 massif, central Vietnam: evidence for East Asia juxtaposition at ca. 250 Ma.
22
23 *Gondwana Research* 4, 720-723.

24
25
26
27
28 Osanai, Y., Nakano, N., Owada, M., Tran Ngoc Nam, Toyoshima, T., Tsunogae, T.,
29
30 and Pham Binh, 2004. Permo-Triassic ultrahigh-temperature metamorphism in the
31
32 Kontum massif, central Vietnam. *Journal of Mineralogical and Petrological Sciences*
33
34 106, 13-25.

35
36
37
38
39 Owada, M., Osanai, Y., Nakano, N., Tran N. Nam, Binh, P., Tsunogae, T., Toyoshima,
40
41 T., Kagami, H., 2007. Crustal anatexis and formation of two types of granitic magmas
42
43 in the Kontum massif, Central Vietnam: Implications for magma processes in
44
45 collision zone. *Gondwana Research* 12, 428-437.

46
47
48
49
50 Pearce, J. A. 1983. Role of the sub-continental lithosphere in magma genesis at active
51
52 continental margins. In: Hawkesworth C. J. & Norry M. J. eds. *Continental Basalts*
53
54 and Mantle Xenoliths, pp. 230–249. Shiva, Nantwich.

55
56
57
58 Peccerillo R, Taylor S R. 1976. Geochemistry of Eocene calc-alkaline volcanic rocks
59
60

1 from the Kastamonu area, Northern Turkey. *Contrib. Mineral Petrol.*, 58: 63~81.
2
3
4 Pham, T. H., Chen, F.K., Nguyen, Thi Bich, Nguyen, Quoc Cuong, Li, S.H., 2013.
5
6 Geochemistry and zircon U–Pb ages and Hf isotopic composition of Permian alkali
7
8
9 granitoids of the Phan Si Pan zone in northwest Vietnam. *Journal of Geodynamics* 69,
10
11
12 106-121.
13
14 Qian, X., Feng, Q., Wang, Y., Chonglakmani, C., Monjai, D., 2015. Geochronological
15
16 and geochemical constraints on the mafic rocks along the Luang Prabang zone:
17
18
19 Carboniferous back-arc setting in northwest Laos. *Lithos*, doi:10.1016 /j.lithos.
20
21
22 2015.07.019.
23
24
25 Racheboeuf, P., Janvier, P., Ta Hoa, P., Vannier, J., Wang, S.Q., 2005. Lower
26
27
28 Devonian vertebrates, arthropods and brachiopods from northern Vietnam. *Geobios*
29
30
31 38, 533–551.
32
33
34 Racheboeuf, P., Ta Hoa, P., Nguyen, H.H., Feist, M., Janvier, P., 2006. Brachiopods,
35
36
37 crustaceans, vertebrates, and charophytes from the Devonian Ly Hoa, Nam Can and
38
39
40 Dong Tho formations of Central Vietnam. *Geodiversitas* 28, 5–36.
41
42
43 Roger, F., Jolivet, M., Maluski, H., Respaut, J., Müncha, P., Paquette, J., Vu Vand, T.,
44
45
46 Nguyen Van, V., 2014. Emplacement and cooling of the Dien Bien Phu granitic
47
48
49 complex: Implications for the tectonic evolution of the Dien Bien Phu Fault (Truong
50
51
52 Son Belt, NW Vietnam). *Gondwana Research* 26: 785–801.
53
54
55 Seneda, A. J., Abrão, A., Dias, S. M., Sato, K., Kakazu, H. M., Salvador, L. R. V.,
56
57
58 Queiroz, A. S. C., da Rocha, M. R. S., Pedreira, R. W., 2009. Radiogenic lead-208
59
60
61 abundance 88.34%. *International Nuclear Atlantic Conference*.

1 Sengör, A.M.C., 1979. Mid-Mesozoic closure of Permo-Triassic Tethys and its
2
3 implications. *Nature* 279, 590-593.
4

5
6 Sengor, A.M.C., Hsu, K.J., 1984. The Cimmerides of eastern Asia: history of the
7
8 eastern end of Paleo-tethys. *Mem. Soc. Geol. Fr.* 147, 139– 167.
9

10
11 Sanematsu, K., Murakam, H., Duangsurigna, S., Vilayhack, S., Duncan, R., and
12
13 Watanabe, Y., 2011. $^{40}\text{Ar}/^{39}\text{Ar}$ ages of granitoids from the Truong Son fold belt and
14
15 Kontum massif in Laos. *Journal of Mineralogical and Petrological Sciences* 106,
16
17 13-25.
18
19

20
21
22 Searle, M.P., Whitehouse, M. J., Robb, J., Ghani, A. A., Hutchison, C.S., Sone, M.,
23
24 Ngi, S. W., Roseiee, M. H., Chung, S. L. and Oliver, G. J. H., 2012. Tectonic
25
26 evolution of the Sibumasu - Indochina terrane collision zone in Thailand and
27
28 Malaysia: constraints from new U–Pb zircon chronology of SE Asian tin granitoids.
29
30
31 *Journal of the Geological Society, London, Vol. 169, 2012, pp. 489 –500.*
32
33

34
35
36 Shellnutt, J.G., Zhou, M.-F., Zellmer, G., 2009. The role of Fe–Ti oxide
37
38 crystallization in the formation of A-type granitoids with implications for the Daly
39
40 gap: an example from the Permian Baima Igneous Complex. *Chemical Geology* 259,
41
42 204–217.
43
44

45
46
47 Shellnutt, J.G., Zhou, M.-F., 2007. Permian peralkaline, peraluminous and
48
49 metaluminous A-type granites in the Panxi district, SW China: their relationship to
50
51 the Emeishan mantle plume. *Chemical Geology* 243, 286–316.
52
53

54
55
56 Singharajwarapan, S., Berry, R., 2000. Tectonic implications of the Nan Suture Zone
57
58 and its relationship to the Sukhothai Fold Belt, Northern Thailand. *Journal of Asian*
59
60

1 Earth Sciences 18, 663–673.

2
3 Sone, M., Metcalfe, I., 2008. Parallel Tethyan suture in mainland Southeast Asia:
4
5
6 New insights from Paleo-Tethys closure and implications for the Indosinian orogeny.
7
8
9 Comptes Rendus Geoscience 340, 166–179.

10
11 Song, X.Y., Zhou, M.-F., Hou, Z.Q., Cao, Z.M., Wang, Y., Li, Y., 2001. Geochemical
12
13
14 constraints on the mantle source of the Upper Permian Emeishan continental flood
15
16
17 basalts, southwestern China. International Geology Review 43, 213–225.

18
19
20 Streckeisen, A., 1967. Classification and nomenclature of igneous rocks. Final report
21
22
23 of an inquiry. Neues Jahrbuch für Mineralogie Abhandlungen 107, 144–204.

24
25 Sun, S. S, McDonough, W. F., 1989. Chemical and isotopic systematics of oceanic
26
27
28 basalts: Implications for mantle composition and processes [M].In: Saunders A D,
29
30
31 Norry M J, eds. Magmatism in the Ocean Basins. Geological Society, London,
32
33
34 Special Publications, 42: 313-345.

35
36 Tran, H. T., Khin, Zaw., Halpin, J., Manaka, T., Meffre, S., Lai, C.K., Lee, Y.J., Le,
37
38
39 V. H., Dinh, S., 2014. The Tam Ky–Phuoc Son Shear Zone in Central Vietnam:
40
41
42 tectonic and metallogenic implications. Gondwana Research 26 (1), 144–164.

43
44 Ueno, K., 2003. The Permian fusulinoidean faunas of the Sibumasu and Baoshan
45
46
47 blocks: their implications for the paleogeographic and paleoclimatologic
48
49
50 reconstruction of the Cimmerian continent. Palaeogeography, Palaeoclimatology,
51
52
53 Palaeoecology 193, 1-24.

54
55 Wang, X., Metcalfe, I., Jian P., He, L., Wang, C., 2000. The Jinshajiang–Ailaoshan
56
57
58 suture zone, China: tectonostratigraphy, age and evolution. Journal of Asian Earth
59
60

1 Sciences 18 (6), 675-690.

2
3 Wang, C.Y., Zhou, M. F., Qi, L., 2007. Permian flood basalts and mafic intrusions in
4 the Jinping (SW China)–Song Da (northern Vietnam) district: mantle sources, crustal
5 contamination and sulfide segregation. *Chemical Geology* 243, 317–343.

6
7
8
9 Wang, E., Burchfiel, B. C., Royden, L. H., Chen, L., Chen, J., Li, W., Chen, Z., 1998.
10 Late Cenozoic Xianshuihe-Xiaojiang, Red River, and Dali fault systems of
11 southwestern Sichuan and central Yunnan, China. *Geology Society of American*
12 *Special Paper* 327, p. 108.

13
14
15
16
17
18
19
20 Whalen J.B., Currie K.L., Chappell B.W.1987. A-type granites: geochemical
21 characteristics, discrimination and petrogenesis. *Contributions to Mineralogy and*
22 *Petrology* 95, 407-419.

23
24
25
26
27
28
29
30 Wu, F.Y., Yang, Y.H., Xie, L.W., Yang, J.H., Xu, P., 2006. Hf isotopic compositions
31 of the standard zircons and baddeleyites used in U–Pb geochronology. *Chemical*
32 *Geology* 234, 105-126.

33
34
35
36
37
38
39
40
41
42
43
44
45
46 Wu, H., Boulter, C.A., Ke, B., Stow, D.A.V., Wang, Z., 1995. The
47 Changning-Menglian suture zone; a segment of the major Cathaysian –Gondwana
48 divide in Southeast Asia. *Tectonophysics* 242, 267–280.

49
50
51
52
53
54
55
56
57
58
59
60
61
62
63
64
65
66
67
68
69
70
71
72
73
74
75
76
77
78
79
80
81
82
83
84
85
86
87
88
89
90
91
92
93
94
95
96
97
98
99
100
101
102
103
104
105
106
107
108
109
110
111
112
113
114
115
116
117
118
119
120
121
122
123
124
125
126
127
128
129
130
131
132
133
134
135
136
137
138
139
140
141
142
143
144
145
146
147
148
149
150
151
152
153
154
155
156
157
158
159
160
161
162
163
164
165
166
167
168
169
170
171
172
173
174
175
176
177
178
179
180
181
182
183
184
185
186
187
188
189
190
191
192
193
194
195
196
197
198
199
200
201
202
203
204
205
206
207
208
209
210
211
212
213
214
215
216
217
218
219
220
221
222
223
224
225
226
227
228
229
230
231
232
233
234
235
236
237
238
239
240
241
242
243
244
245
246
247
248
249
250
251
252
253
254
255
256
257
258
259
260
261
262
263
264
265
266
267
268
269
270
271
272
273
274
275
276
277
278
279
280
281
282
283
284
285
286
287
288
289
290
291
292
293
294
295
296
297
298
299
300
301
302
303
304
305
306
307
308
309
310
311
312
313
314
315
316
317
318
319
320
321
322
323
324
325
326
327
328
329
330
331
332
333
334
335
336
337
338
339
340
341
342
343
344
345
346
347
348
349
350
351
352
353
354
355
356
357
358
359
360
361
362
363
364
365
366
367
368
369
370
371
372
373
374
375
376
377
378
379
380
381
382
383
384
385
386
387
388
389
390
391
392
393
394
395
396
397
398
399
400
401
402
403
404
405
406
407
408
409
410
411
412
413
414
415
416
417
418
419
420
421
422
423
424
425
426
427
428
429
430
431
432
433
434
435
436
437
438
439
440
441
442
443
444
445
446
447
448
449
450
451
452
453
454
455
456
457
458
459
460
461
462
463
464
465
466
467
468
469
470
471
472
473
474
475
476
477
478
479
480
481
482
483
484
485
486
487
488
489
490
491
492
493
494
495
496
497
498
499
500
501
502
503
504
505
506
507
508
509
510
511
512
513
514
515
516
517
518
519
520
521
522
523
524
525
526
527
528
529
530
531
532
533
534
535
536
537
538
539
540
541
542
543
544
545
546
547
548
549
550
551
552
553
554
555
556
557
558
559
560
561
562
563
564
565
566
567
568
569
570
571
572
573
574
575
576
577
578
579
580
581
582
583
584
585
586
587
588
589
590
591
592
593
594
595
596
597
598
599
600
601
602
603
604
605
606
607
608
609
610
611
612
613
614
615
616
617
618
619
620
621
622
623
624
625
626
627
628
629
630
631
632
633
634
635
636
637
638
639
640
641
642
643
644
645
646
647
648
649
650
651
652
653
654
655
656
657
658
659
660
661
662
663
664
665
666
667
668
669
670
671
672
673
674
675
676
677
678
679
680
681
682
683
684
685
686
687
688
689
690
691
692
693
694
695
696
697
698
699
700
701
702
703
704
705
706
707
708
709
710
711
712
713
714
715
716
717
718
719
720
721
722
723
724
725
726
727
728
729
730
731
732
733
734
735
736
737
738
739
740
741
742
743
744
745
746
747
748
749
750
751
752
753
754
755
756
757
758
759
760
761
762
763
764
765
766
767
768
769
770
771
772
773
774
775
776
777
778
779
780
781
782
783
784
785
786
787
788
789
790
791
792
793
794
795
796
797
798
799
800
801
802
803
804
805
806
807
808
809
810
811
812
813
814
815
816
817
818
819
820
821
822
823
824
825
826
827
828
829
830
831
832
833
834
835
836
837
838
839
840
841
842
843
844
845
846
847
848
849
850
851
852
853
854
855
856
857
858
859
860
861
862
863
864
865
866
867
868
869
870
871
872
873
874
875
876
877
878
879
880
881
882
883
884
885
886
887
888
889
890
891
892
893
894
895
896
897
898
899
900
901
902
903
904
905
906
907
908
909
910
911
912
913
914
915
916
917
918
919
920
921
922
923
924
925
926
927
928
929
930
931
932
933
934
935
936
937
938
939
940
941
942
943
944
945
946
947
948
949
950
951
952
953
954
955
956
957
958
959
960
961
962
963
964
965
966
967
968
969
970
971
972
973
974
975
976
977
978
979
980
981
982
983
984
985
986
987
988
989
990
991
992
993
994
995
996
997
998
999
1000

1 determination of trace elements, U–Pb and Lu–Hf isotopes in zircon and baddeleyite.

2
3 Chinese Science Bulletin 53, 1565–1573.

4
5
6 Xu, Y., Chung, S.L., Jahn, B.M., Wu, G., 2001. Petrologic and geochemical
7
8 constraints on the petrogenesis of Permian–Triassic Emeishan flood basalts in
9
10 southwestern China. *Lithos* 58, 145–168.

11
12
13
14
15
16
17 Zhou, M.-F., Zhao, J.H., Qi, L., Su, W.C., Hu, R.Z., 2006. Zircon U–Pb
18
19 geochronology and elemental and Sr–Nd isotope geochemistry of Permian mafic
20
21 rocks in the Funing area, SW China. *Contrib. Mineral. Petrol.* 151, 1–19.

22
23
24
25 Zuchiewicz, W., Cuong, N. Q., Bluszcz, A., and Michalik, M. 2004. Quaternary
26
27 sediments in the Dien Bien Phu fault zone, NW Vietnam: a record of young tectonic
28
29 processes in the light of OSL-SAR dating results. *Geomorphology* 60:269–302.

30
31
32
33
34 Zhai, Q., Jahn, B., Su, L., Wang, J., Mo, X., Lee, H., Wang, K., Tang, S., 2012.
35
36 Triassic arc magmatism in the Qiangtang area, northern Tibet: zircon U–Pb ages,
37
38 geochemical and Sr–Nd–Hf isotopic characteristics, and tectonic implications. *Journal*
39
40
41
42 of *Asian Earth Sciences* 63, 162–178.

43
44
45 Zhang, L., Ding, Lin., Pullen, Alex., Xu, Q., Liu, D., Cai, F., Yue, Y., Lai, Q., Shi, R.,
46
47 Ducea, M., Kapp, P., Chapman, A., 2014. Age and geochemistry of western
48
49 Hoh-Xil–Songpan–Ganzi granitoids, northern Tibet: Implications for the Mesozoic
50
51
52
53 closure of the Paleo-Tethys ocean. *Lithos* 190–191, 328–348.

1 **Captions:**
2

3 Figure 1 Distribution of principal continental terranes and sutures of Mainland SE
4
5 Asia (After Sone and Metcalfe, 2008). C. M. S. Z= Changning-Menglian Suture zone,
6
7 the locations of Figures 2 & 3 are also shown.
8
9

10
11
12 Figure 2 Distribution of strata and granite complexes in northern Laos. Locations of
13
14 granite samples are also shown (after DGM, 1991).
15
16
17

18
19
20 Figure 3 Cross-section of the Song Ma Suture Zone shows the simplified geological
21
22 relation between different tectonic units eastward from the Indochina Block to the
23 South China Block.
24
25
26
27

28
29
30 Figure 4 Cathodoluminescence (CL) images of representative zircon grains and zircon
31
32 age concordia diagrams of granites from northern Laos.
33
34
35
36

37 Figure 5 Plot of $\epsilon_{\text{Hf}}(t)$ vs. U–Pb ages for granites from northern Laos.
38
39
40
41

42 Figure 6 Modal classification of granitoids (after Streckeisen, 1967). Granites from
43 the Lat Boua, Laosang and Kham complexes mainly in the monzogranite field;
44 granites from the Phon Thong, Na The, and Luu complexes in the granodiorite field;
45 two samples from the Luu complex in the tonalite field. 1-alkali feldspar syenite;
46 2-syenite; 3-monzonite; 4-monzodiorite; 5- diorite; 6-quartz alkali feldspar syenite;
47
48
49
50
51
52
53
54
55
56
57
58
59
60

1 7-quartz syenite; 8-adamellite; 9- quartz monzobiorite; 10- quartz diorite; 11- alkalic
2
3 feldspar granite; 12- syengranite; 13-monzogranite; 14-granodiorite; 15-tonalite;
4
5
6 16-quartz granite; 17- quartzite
7
8
9

10
11 Figure 7 Plots of (a) K_2O vs. SiO_2 (solid line after Peccerillo and Taylor, 1976; dash
12
13 line after Middlemost, 1985) and (b) A/NK vs. A/CNK (after Maniar and Piccoli,
14
15 1989) for granites from northern Laos. $A = Al_2O_3$, $N = Na_2O$, $K = K_2O$, $C = CaO$ (all
16
17 in molar proportion).
18
19
20
21
22
23
24

25 Figure 8 Chondrite-normalized REE patterns (Boynnton, 1984) and primitive-mantle
26
27 normalized trace element patterns for I-type granites in northern Laos (Sun and
28
29 McDonough, 1989).
30
31
32
33
34
35

36 Figure 9 Th/Yb vs. Ta/Yb diagram (Pearce, 1983) and Hf -Rb-Ta discrimination
37
38 diagram (Harris *et al.*, 1986) identifying tectonic setting.
39
40
41
42
43

44 Figure 10 (Na_2O+K_2O) vs. $(Zr+Nb+Ce+Y)$ diagram (Whalen *et al.*, 1987) and Th vs.
45
46 Rb diagram (Chappell *et al.*, 1992) identifying I-S type granites.
47
48
49
50
51
52

53 Figure 11 Paleogeographic reconstructions of the Tethyan region in the Late Permian
54
55 to Early Triassic showing relative positions of the east and Southeast Asian blocks
56
57 and distribution of land and sea (after Metcalfe, 2006). Abbreviations: SC=South
58
59
60
61
62
63
64
65

1 China; NC=North China; I=Indochina; QS=Qamdo-Simao; EM=East Malaya;
2
3 S=Sibumasu; WB=West Burma; QI=Qiangtang; L=Lhasa; WC=Western Cimmerian
4
5
6 Continent.
7
8
9

10
11 Figure 12 Geodynamic model of the convergence of the Southeast Asian blocks
12
13 during closure of the Paleotethyan Ocean (after Jian *et al.*, 2009, Liu *et al.*, 2012;
14
15 Faure *et al.*, 2014).
16
17
18
19
20
21

22 Table 4 The whole-rock major element components in the 33 samples from six
23
24 complexes in northern Laos.
25
26
27
28
29

30 **Appendix A: Supplementary data**

31 Table 1 LA-ICPMS U–Pb zircon age data for granites from northern Laos.
32
33
34
35
36
37

38 **Appendix B: Supplementary data**

39 Table 2 Hf isotopic data for zircons from the granite complex.
40
41
42
43
44
45

46 **Appendix C: Supplementary data**

47 Table 3 Major (wt.%), trace (ppm) and rare earth (ppm) elements of granites from the
48
49 northern Laotian complexes.
50
51
52
53
54
55
56
57
58
59
60
61
62
63
64
65

e-component

[Click here to download e-component: Table-1 U-Pb ages.doc](#)

e-component

[Click here to download e-component: Table 2 Lu-Hf.doc](#)

e-component

[Click here to download e-component: Table-3.doc](#)

Figure
[Click here to download high resolution image](#)

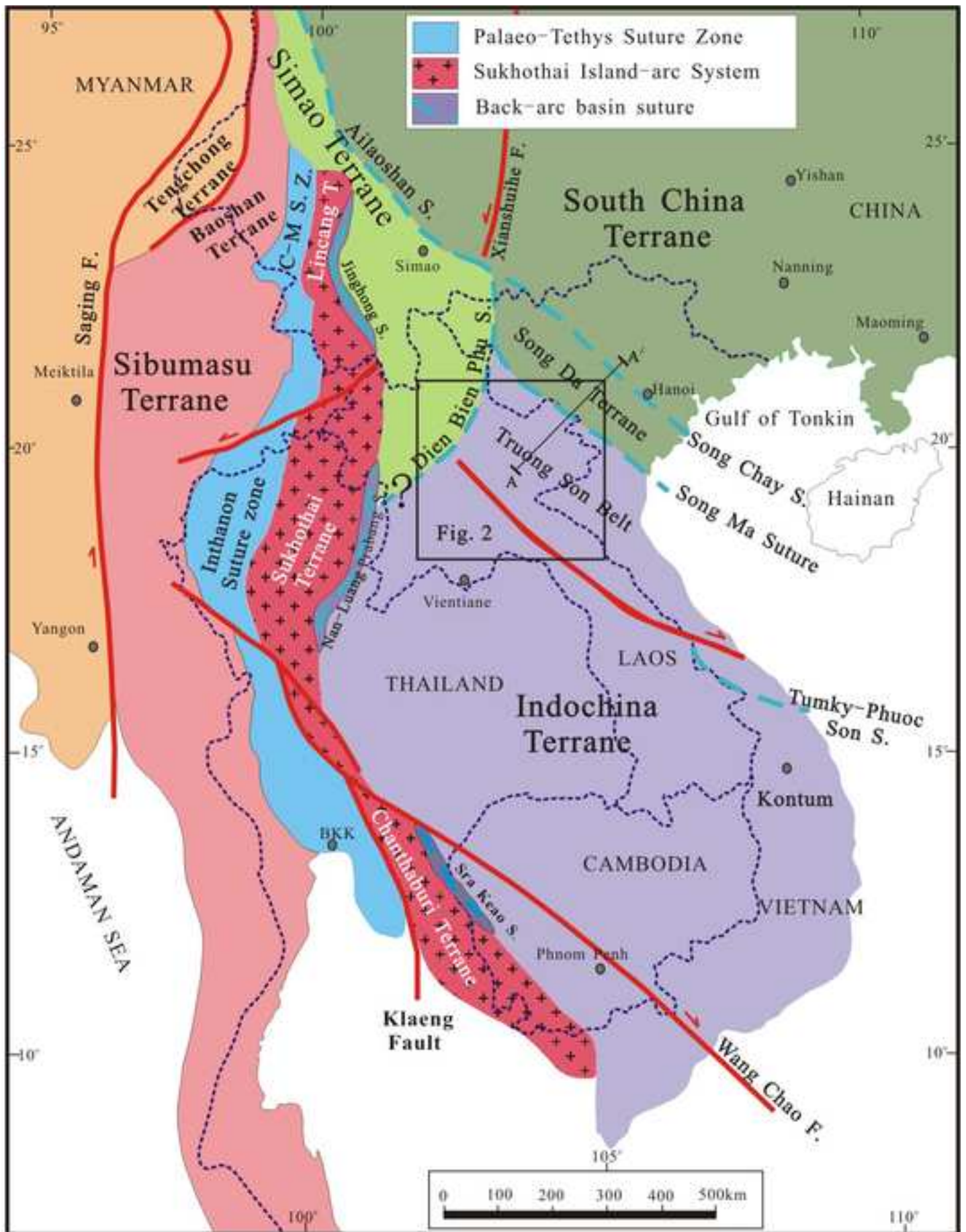


Fig. 1

Figure
[Click here to download high resolution image](#)

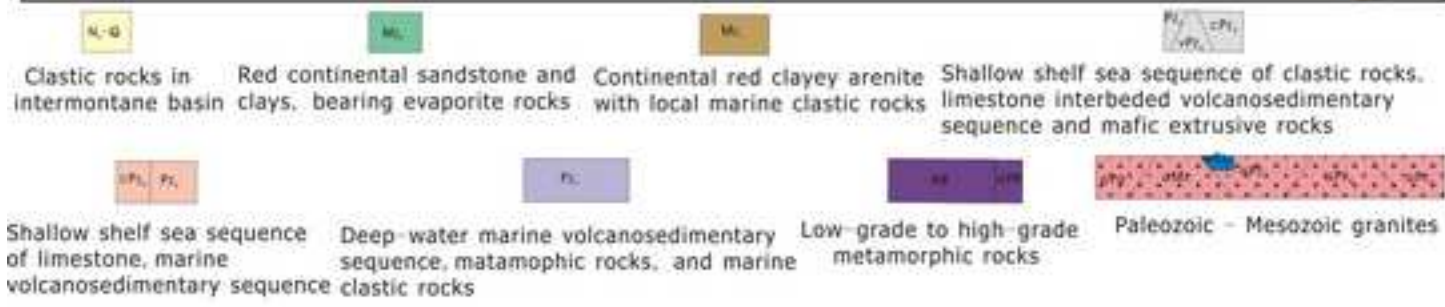
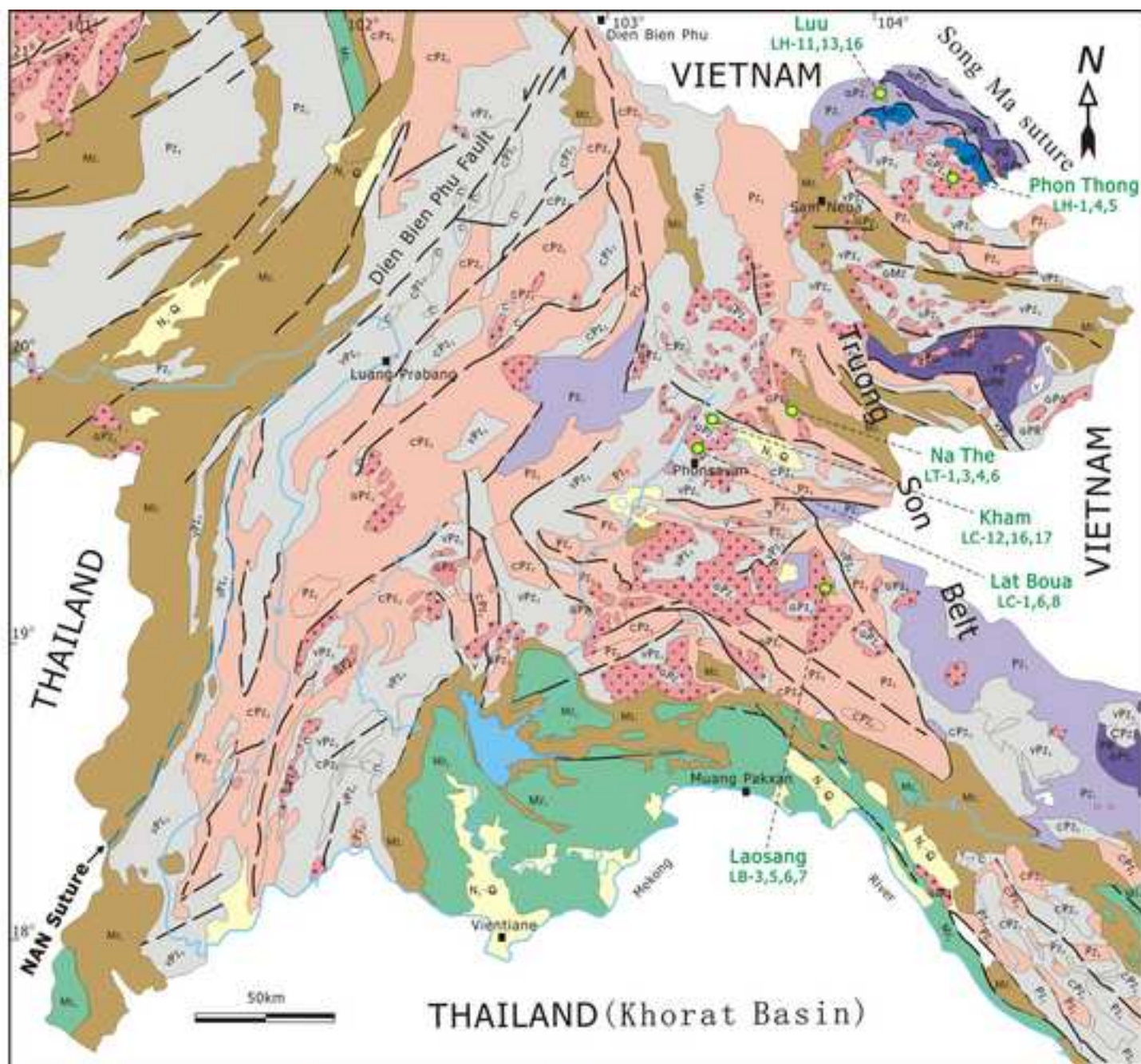


Fig. 2

Figure
[Click here to download high resolution image](#)

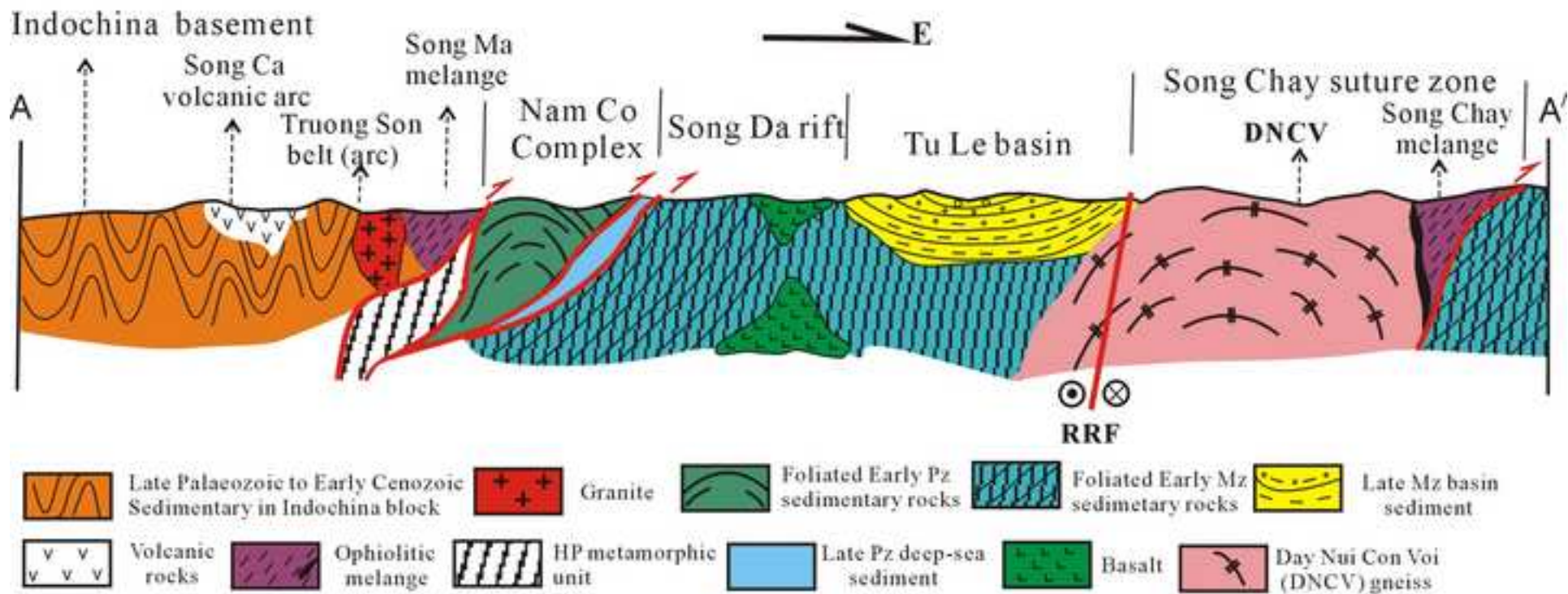


Fig. 3

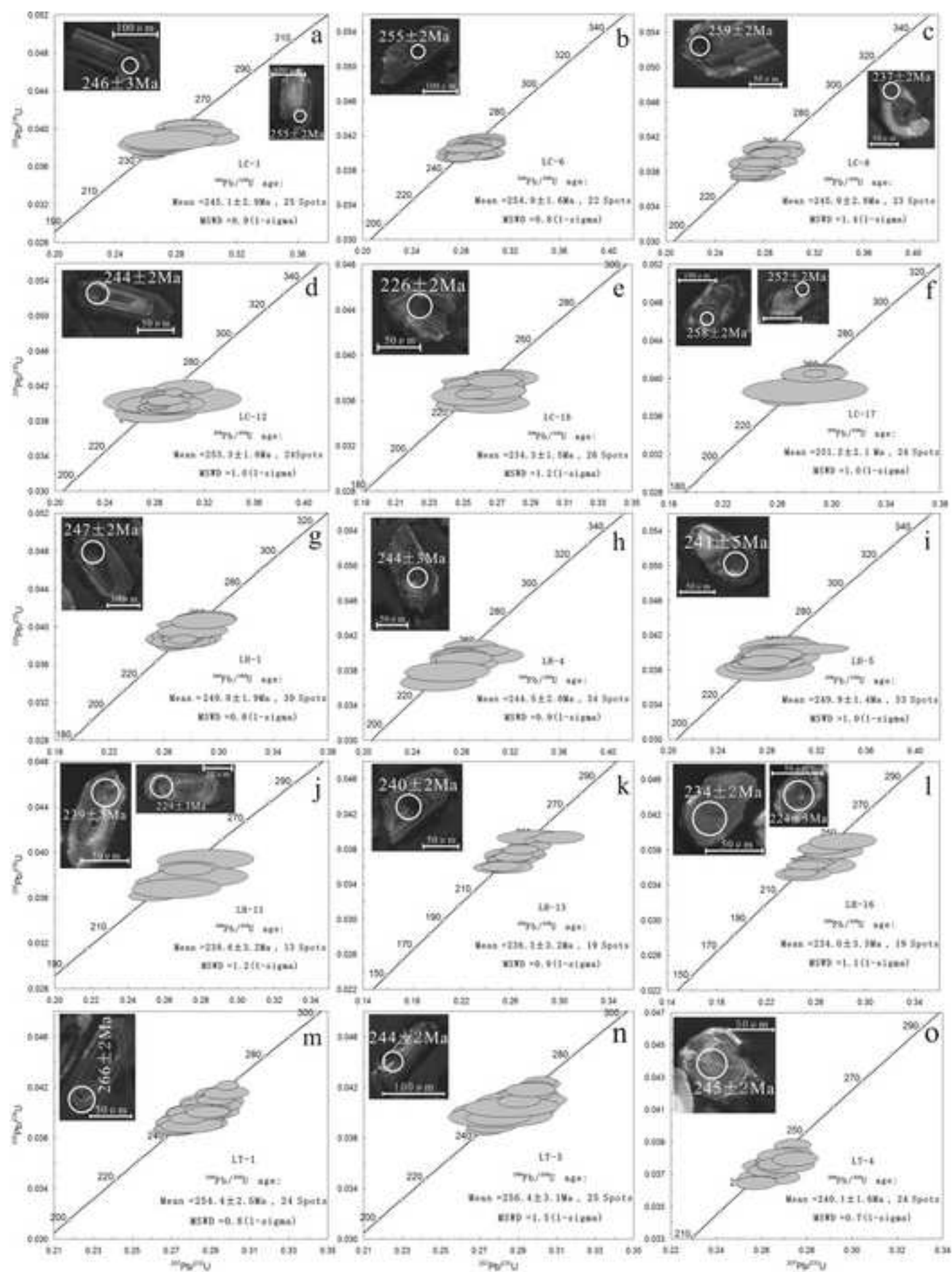


Fig. 4

Figure

[Click here to download high resolution image](#)

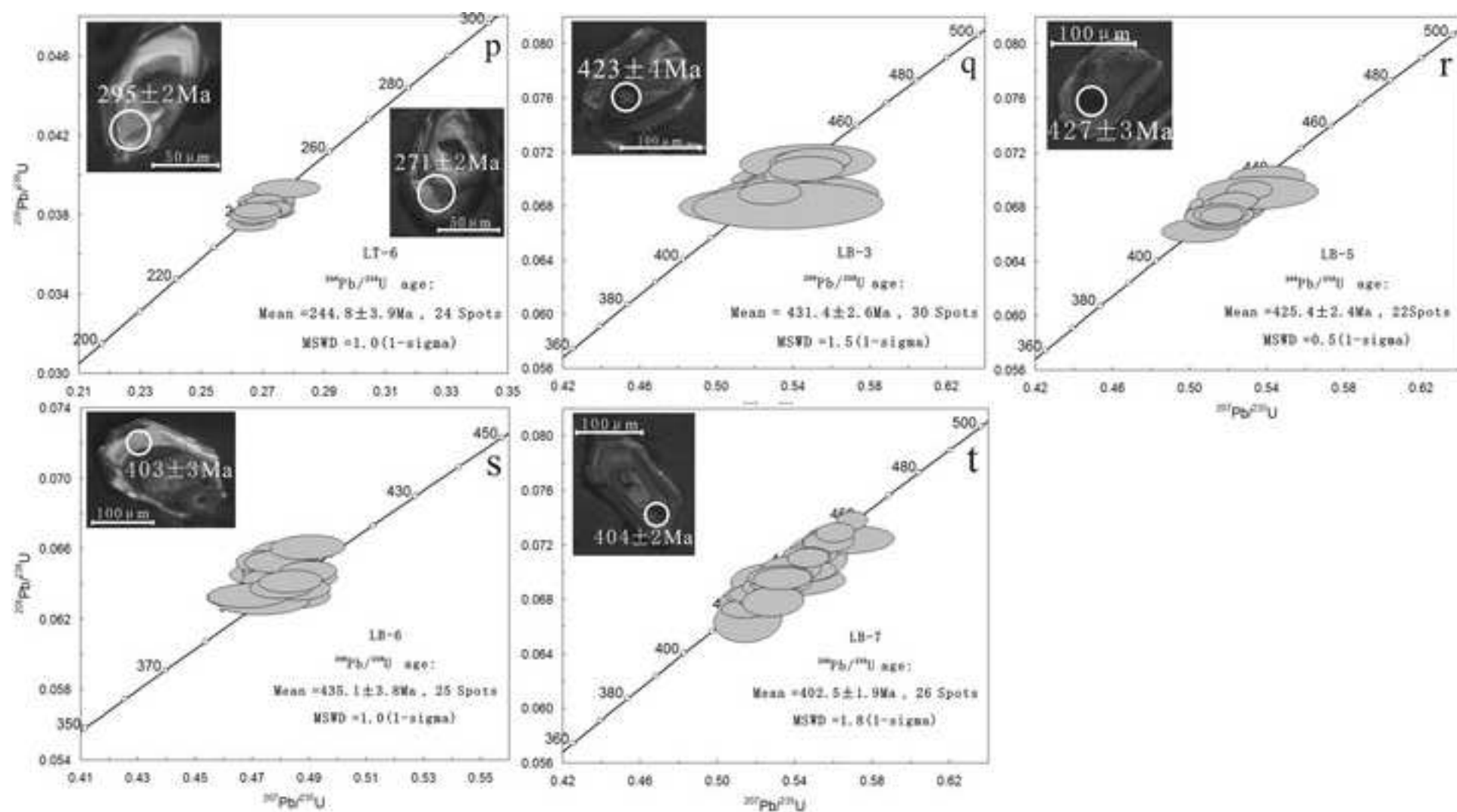


Fig. 4. (continued)

Figure

[Click here to download high resolution image](#)

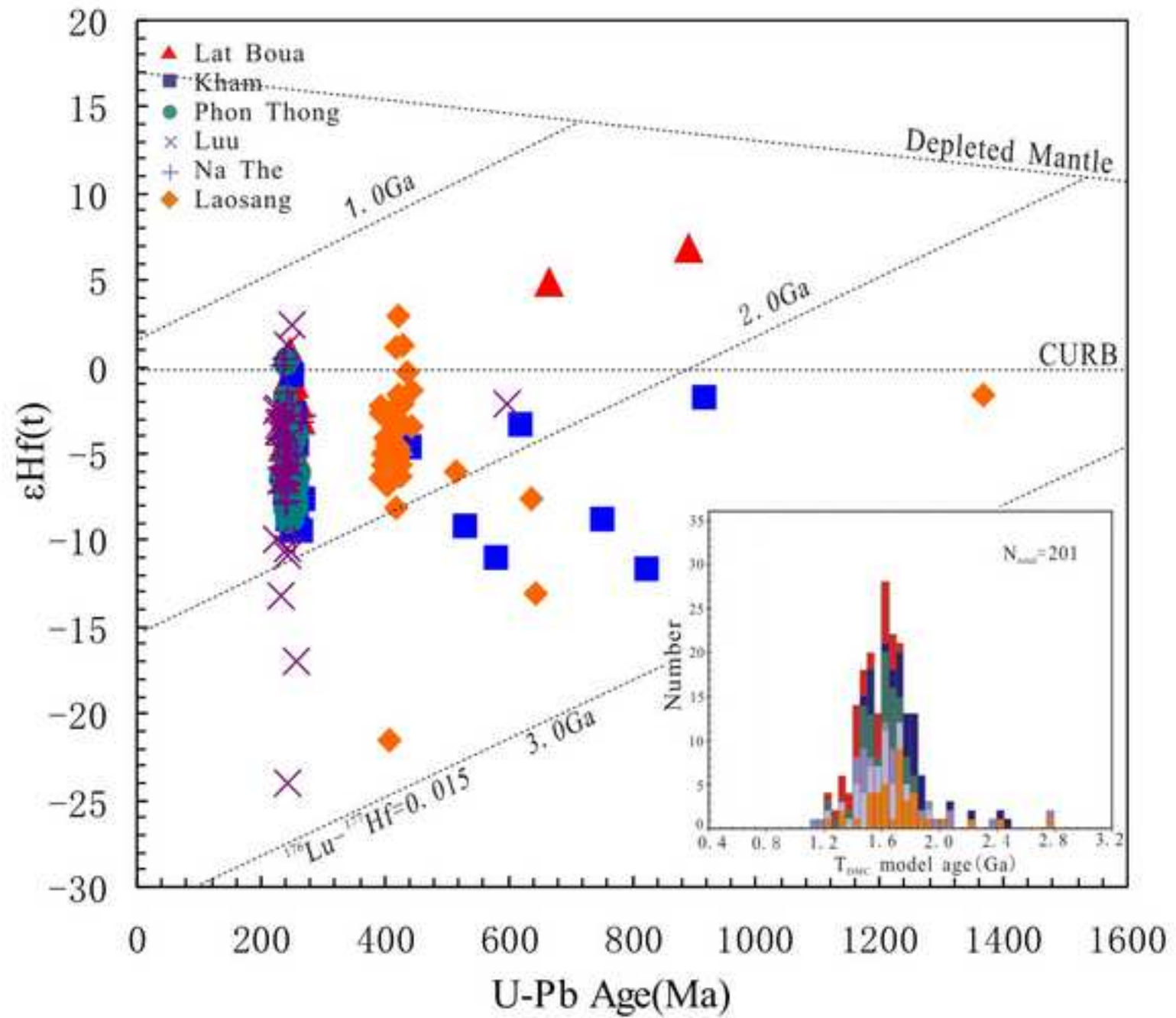


Fig. 5

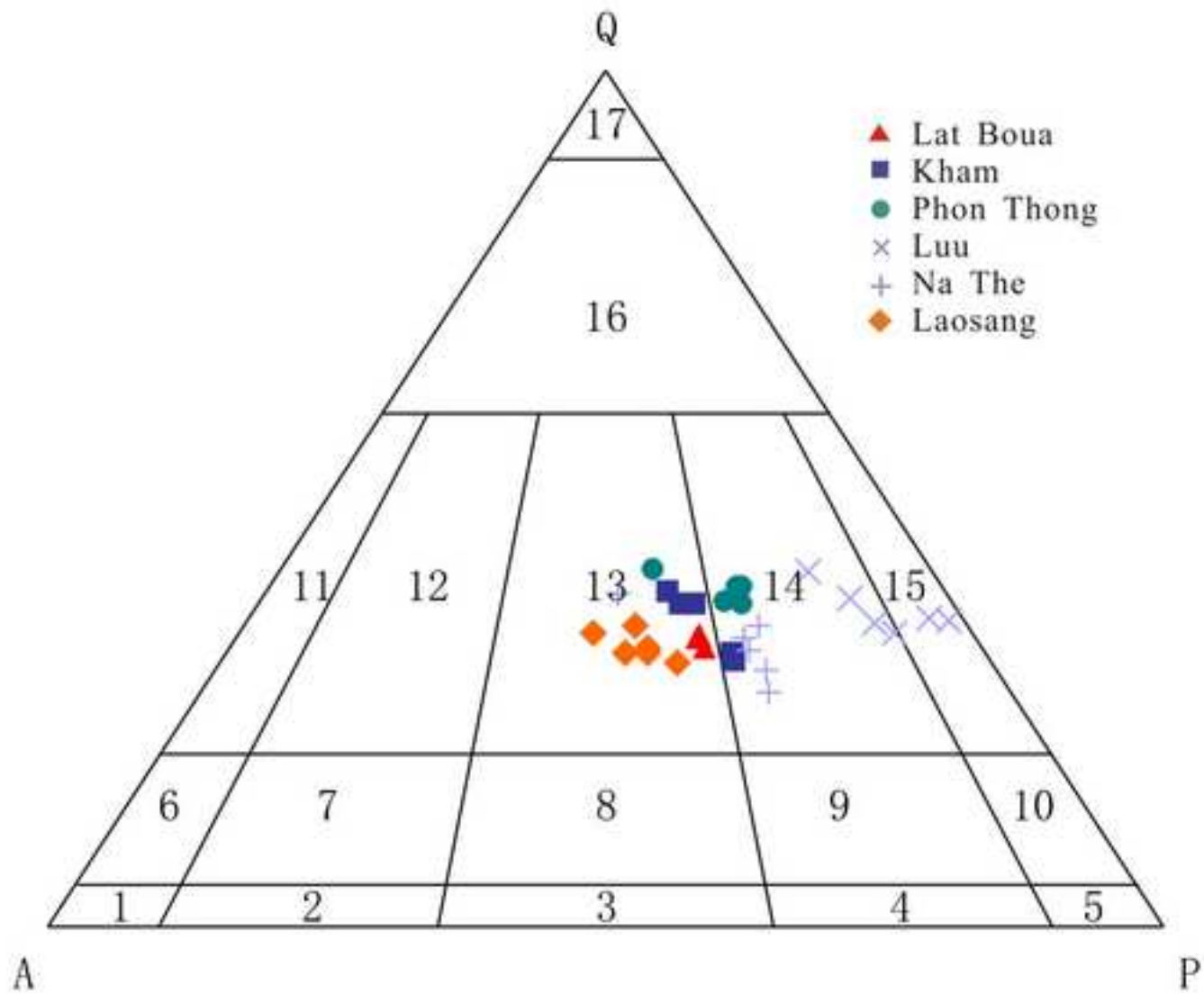


Fig. 6

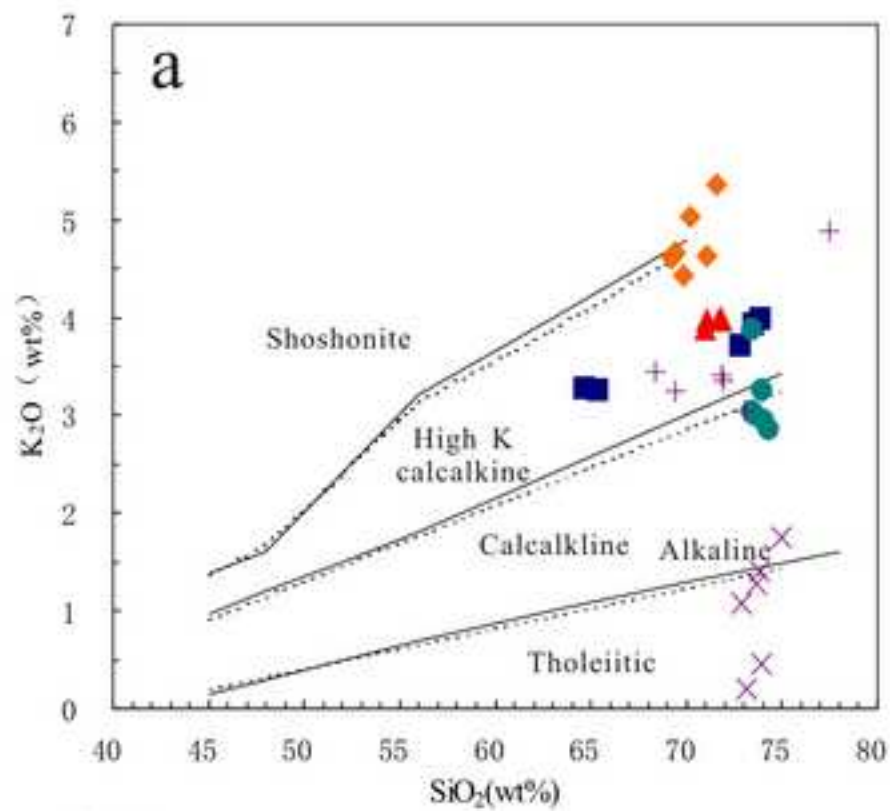
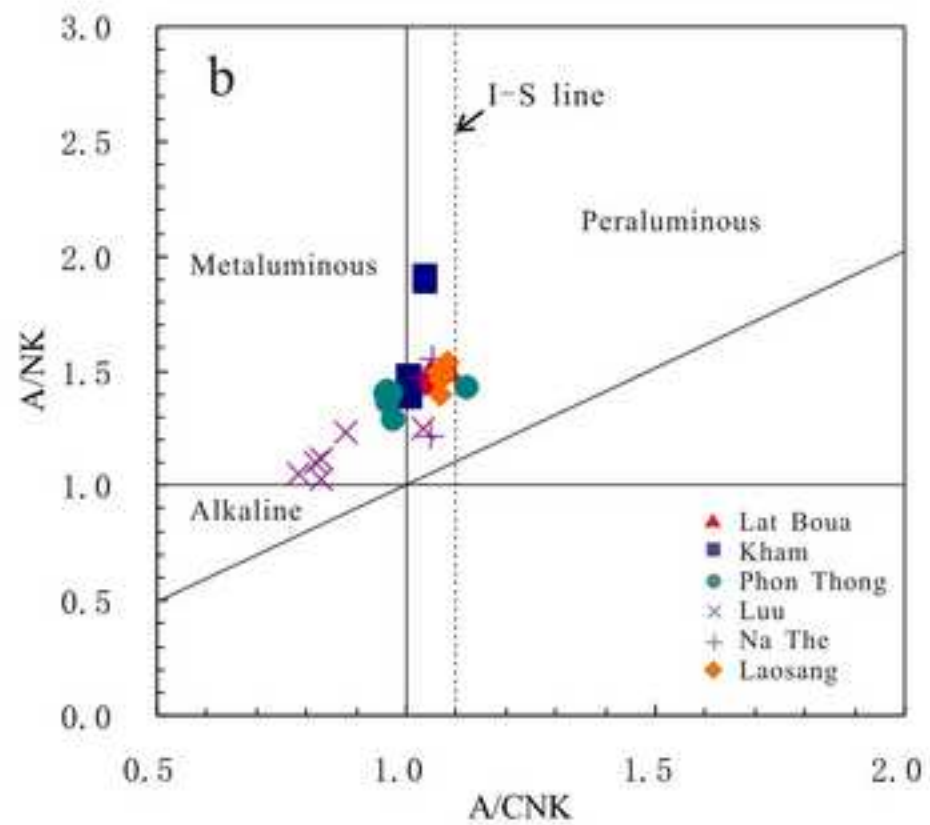


Fig. 7



Figure

[Click here to download high resolution image](#)

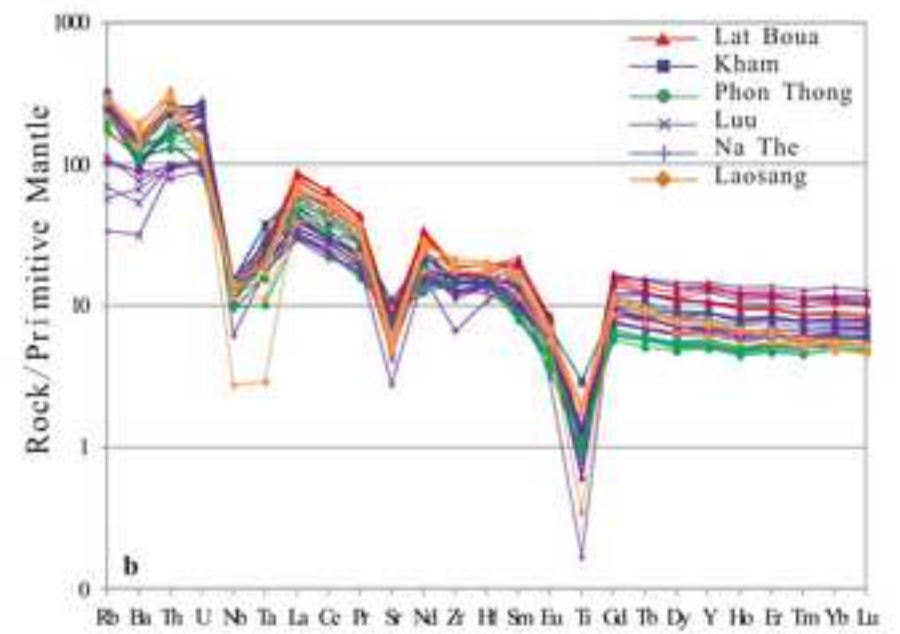
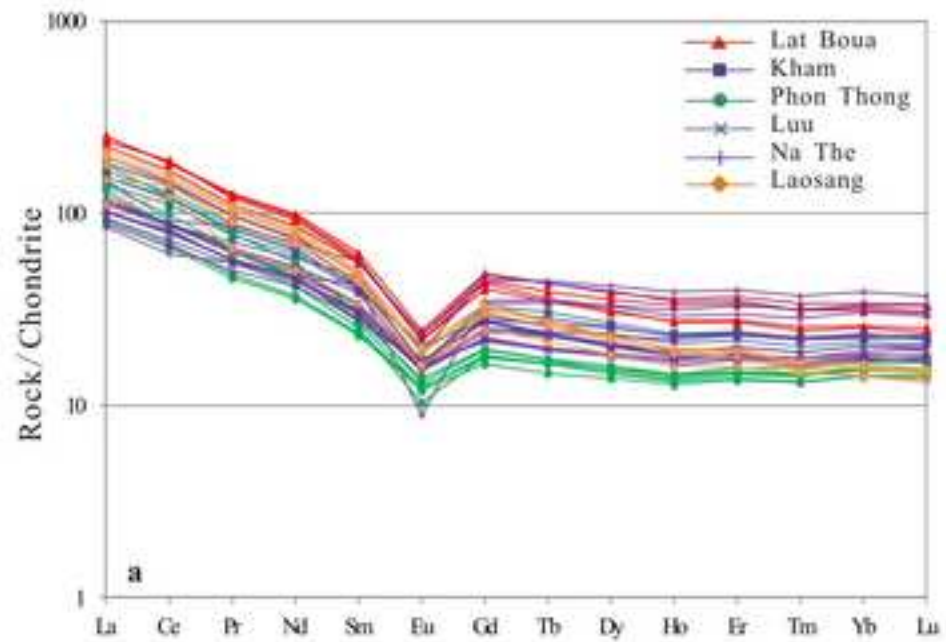


Figure
[Click here to download high resolution image](#)

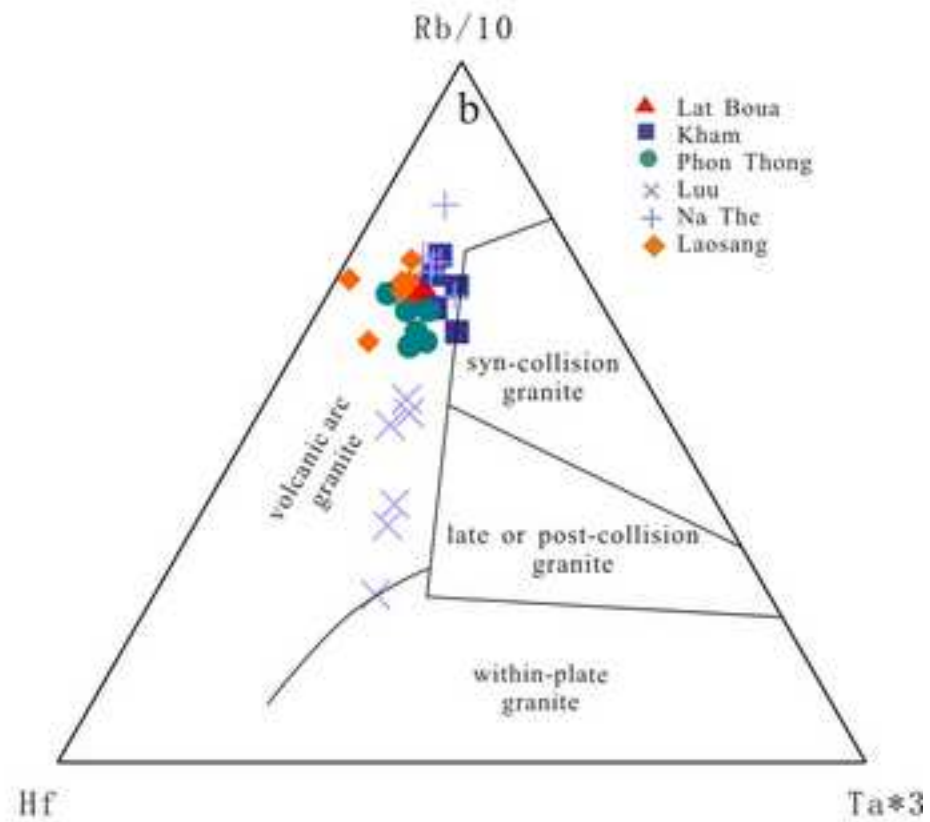
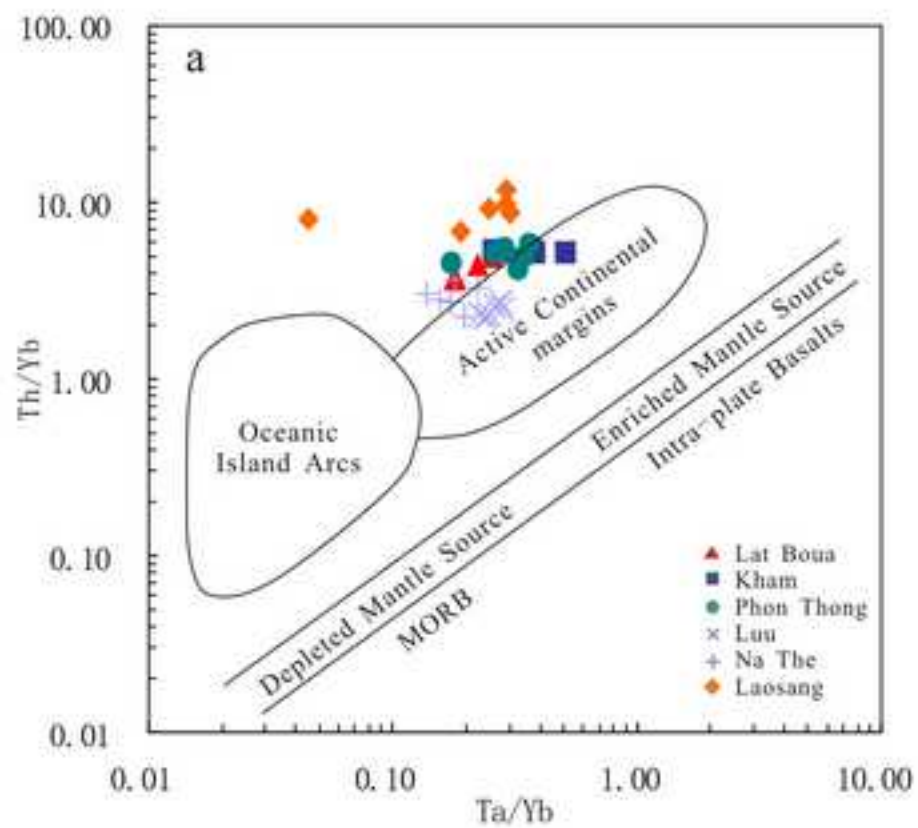


Fig. 9

Figure

[Click here to download high resolution image](#)

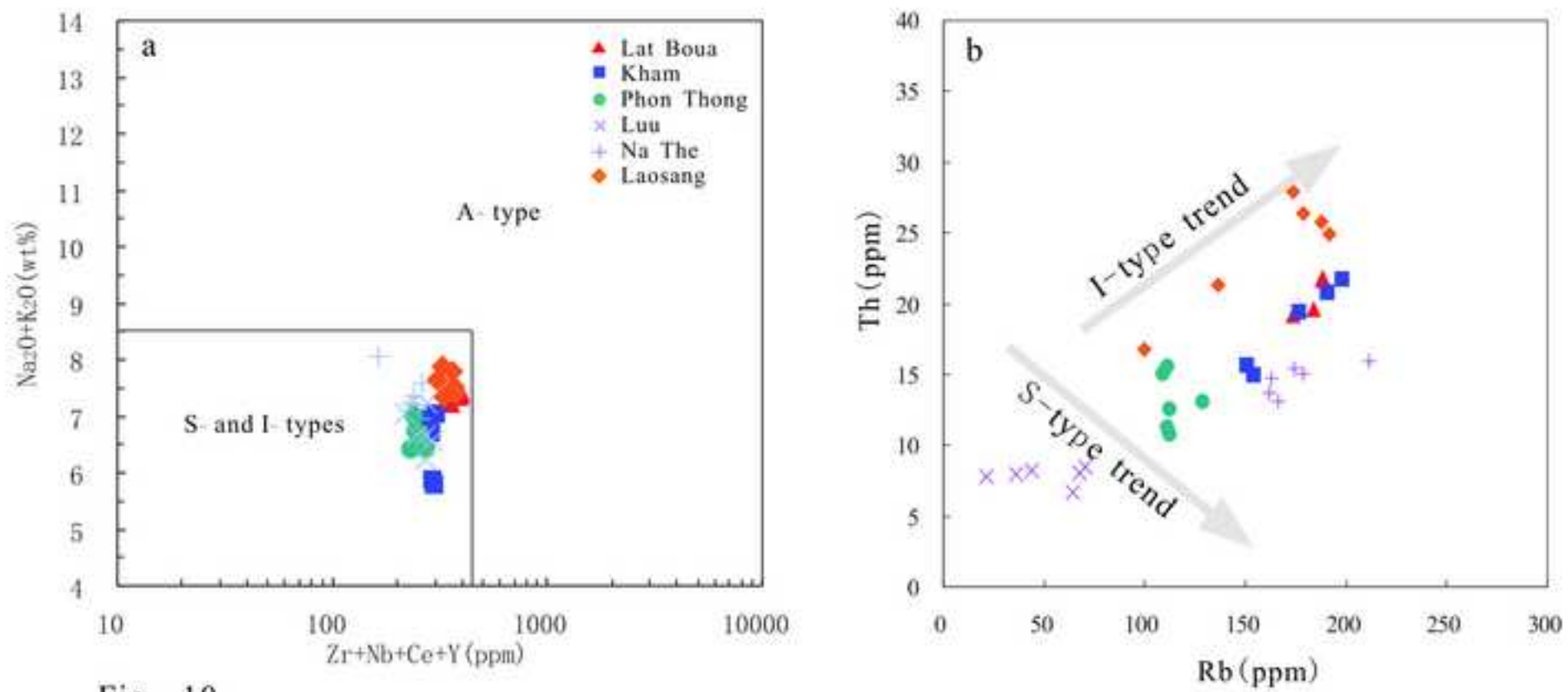


Fig. 10

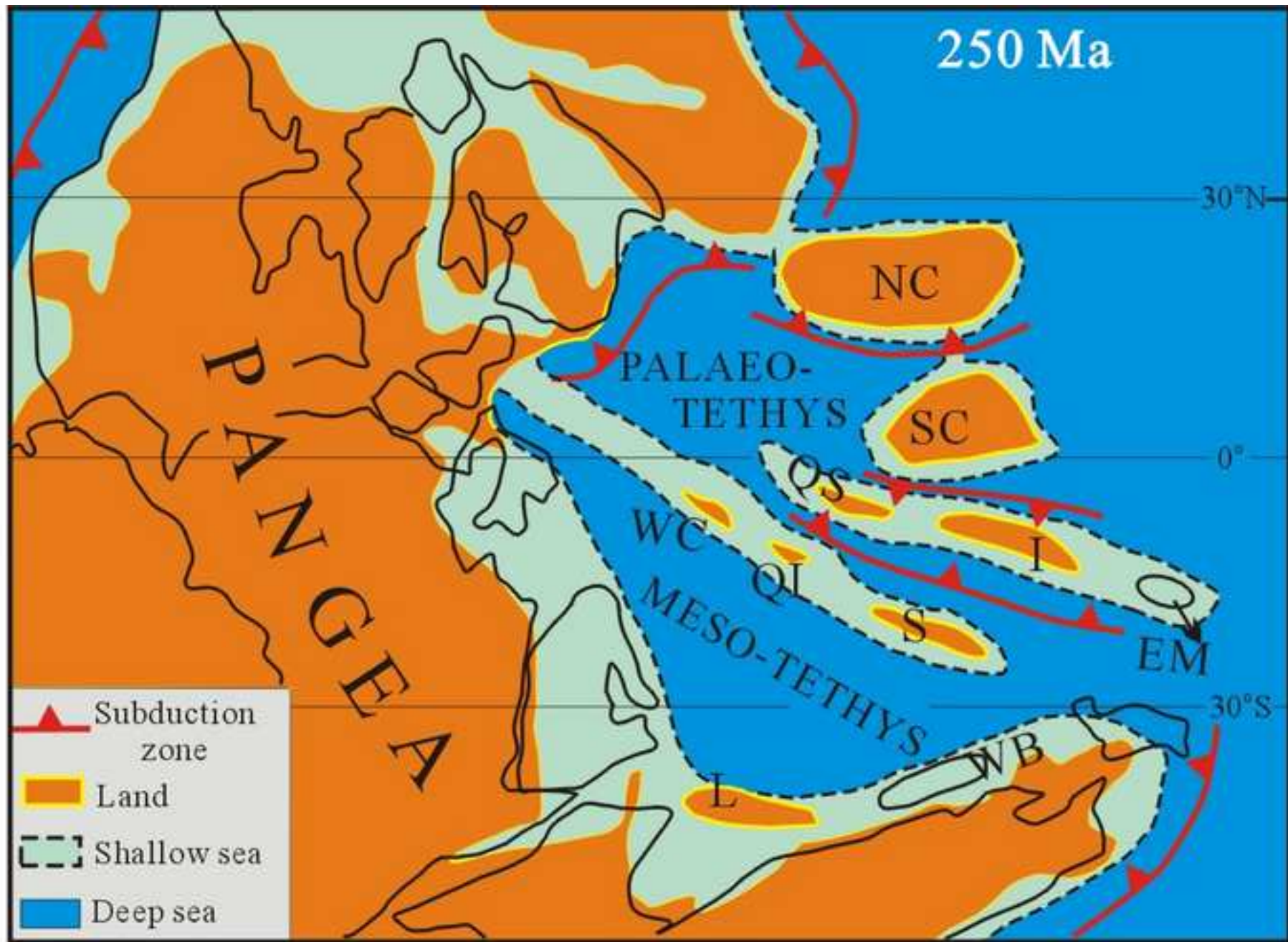


Fig. 11

Figure

[Click here to download high resolution image](#)

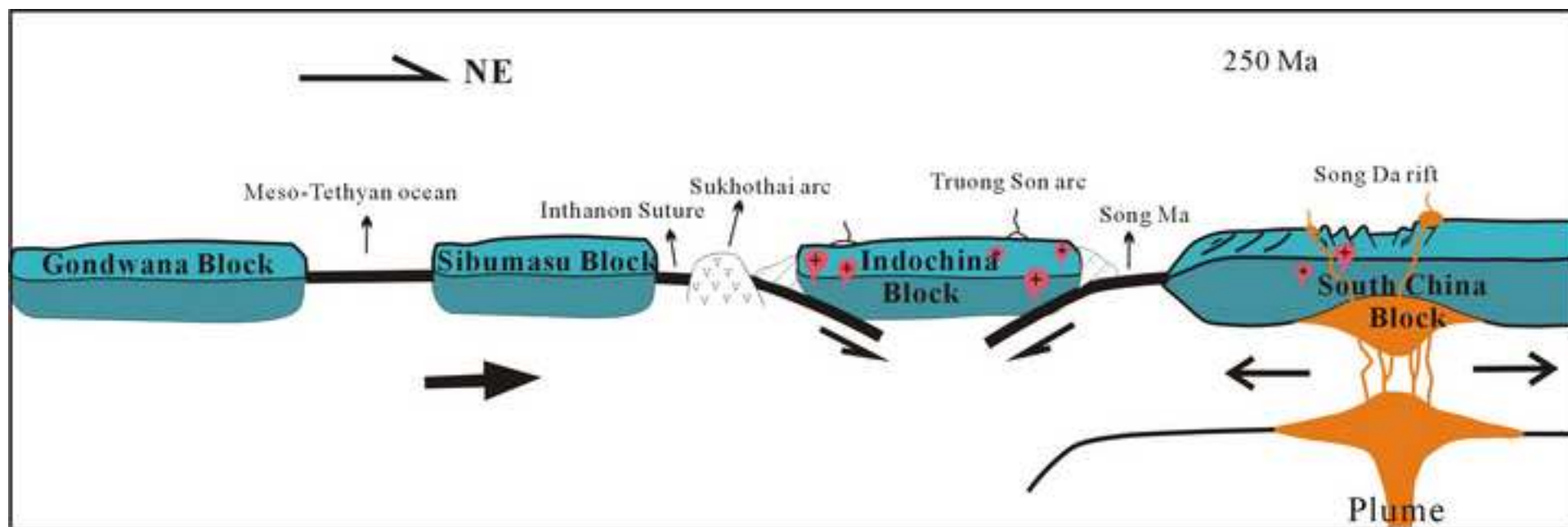


Fig. 12

Table 4

	Lat Boua	Kham	Na The	Phon Thong	Luu	Laosang
SiO ₂ (%)	71-71.8	64.6-73.9	68.4-77.5	73.4-74.3	72.9-75.0	69.2-71.6
Na ₂ O+K ₂ O(%)	7.24-7.41	7.1-7.8	7.0-8.1	6.4-7.1	6.3-7.2	7.4-7.9
K ₂ O/Na ₂ O	1.15-1.19	1.23-1.35	0.78-1.53	0.8-1.36	0.03-0.39	1.39-2.11
Al ₂ O ₃ (%)	14.5-14.8	12.8-14.8	12.8-15.9	12.6-13.0	11.4-12.5	14.0-15.5
Aluminium index	1.04-1.08	1.0-1.04	1.03-1.05	0.96-1.12	0.78-1.03	1.06-1.08
Litman index	1.87-1.96	1.50-1.63	1.61-2.28	1.32-1.59	1.22-1.75	1.92-2.24
Granites	monzogranite	monzogranite	granodiorite	granodiorite	tonalite	monzogranite
Alkalinity	high-K calc-alkaline	high-K calc-alkaline	high-K calc-alkaline	calc-alkaline	low-K	high-K calc-alkaline
Aluminium	peraluminous	peraluminous	peraluminous	meta-aluminous	meta-aluminous	peraluminous